A strand-specific burst in transcription of pericentric satellites is required for chromocenter formation and early mouse development.

Aline V. Probst, Ikuhiro Okamoto, Miguel Casanova, Fatima El-Marjou, Patricia Le Baccon, Geneviève Almouzni

A strand-specific burst in transcription of pericentric satellites is required for chromocenter formation and early mouse development

Probst A. V.[1,5], Okamoto, I.[2,#], Casanova, M.[1,#], ElMarjou, F.[3], Le Baccon, P [1,4] and Almouzni, G. [1,*]

[1] Chromatin Dynamics Group, Institut Curie, Centre National de la Recherche Scientifique, Unité Mixte de Recherche 218–Nuclear Dynamics and Genome Plasticity, 75248 Paris, France

[2] Mammalian Developmental Epigenetics Group, Institut Curie, Centre National Research Scientifique Unité Mixte de Recherche 3215, Institut National de la Santé et de la Recherche Médicale U934, 75248 Paris, France

[3] Morphogenesis and Intracellular Signaling, Institut Curie-Unité Mixte de Recherche 144 Centre National de la Recherche Scientifique, 75248 Paris Cedex 05, France.

[4] PITC-IBiSA (Plateforme Imagerie Tissulaire et Cellullaire), Pavillon Pasteur, Institut Curie, 75248 Paris, France

[5] Present Address: CNRS UMR 6247, INSERM U931, GReD, Clermont Université, 24 Avenue des Landais, 63177 Aubière Cedex, France.

[#] The authors contributed equally to this work.

*Corresponding author: genevieve.almouzni@curie.fr

SUMMARY

At the time of fertilization, the paternal genome lacks the typical configuration and marks characteristic of pericentric heterochromatin. It is thus essential to understand the dynamics of this region during early development, its importance during that time period and how a somatic configuration is attained. Here, we show that pericentric satellites undergo a transient peak in expression precisely at the time of chromocenter formation. This transcription is regulated in a strand-specific manner in time and space and is strongly biased by the parental asymmetry. The transcriptional upregulation follows a developmental clock, yet when replication is blocked chromocenter formation is impeded. Furthermore, interference with major satellite transcripts using LNA-DNA gapmers results in developmental arrest before completion of chromocenter formation. We conclude that the exquisite strand-specific expression dynamics at major satellites during the 2-cell stage, with both up and downregulation, are necessary events for proper chromocenter organization and developmental progression.

INTRODUCTION

During development of a multicellular organism, the organization of the genome into chromatin undergoes important functional changes. Over recent years, much progress has been made in defining the features of chromatin and nuclear organization that contribute to the establishment and propagation of differential gene expression patterns in specific cell lineages (Fraser and Bickmore, 2007; Hemberger et al., 2009). Some of the most impressive changes occur following fertilization, when the different chromatin states acquired during oogenesis and spermatogenesis undergo a series of rearrangements in the zygote so as to allow a return to totipotency. The paternal genome undergoes extensive genome-wide chromatin changes including protamine-histone exchange and active DNA demethylation (Mayer et al., 2000a) and both parental genomes acquire competence to replicate and to activate the zygotic genome within a few hours after fertilization (Bouniol et al., 1995; Worrad et al., 1994). This fundamental developmental transition raises major issues concerning the dynamics of nuclear organization and the setting of epigenetic marks, especially on the paternal genome, which has to establish many chromatin features *de novo*. While keeping a memory of the parental origin of the genome is important in imprinting and dosage compensation (Surani, 2001), the equalization of functional domains, like constitutive heterochromatin, that should behave in a similar fashion in all cell types (Brown, 1966), is also essential. In this context, the pericentromeric regions, as a paradigm of constitutive heterochromatin, are particularly interesting to consider. These domains are localized adjacent to centromeres and play a key role in chromosome segregation (Probst et al., 2009). In most mouse interphase somatic cells, these loci are characterized by a specific chromatin signature and organize in clusters, called chromocenters (Guenatri et al., 2004). However, they can dynamically reorganize during differentiation (Terranova et al., 2005) and adopt a particular organization in specialized cell types like Rod photoreceptor cells (Solovei et al., 2009). At the moment of fertilization, the organization of the pericentric domains, contributed by the two specialized gametes, differs considerably; while maternal pericentric domains are

enriched in histone post-translational modifications typical of somatic cells, the paternal genome is packaged with protamines. Strikingly, during the first cleavage stages paternal pericentric domains lack heterochromatic marks including H3K9me3 or HP1α (Santos et al., 2005) and are instead enriched in members of the Polycomb repressive complex 1 (PRC1) as well as H3K27me3 marks (Puschendorf et al., 2008). The pericentric domains of the two parental origins eventually become equivalent by the 8-cell stage (Merico et al., 2007; Puschendorf et al., 2008). An important question therefore is how the particular heterochromatin state, that is key for cell division, is setup *de novo* on the paternal genome, while the corresponding maternal regions are consolidated.

Transcripts generated by pericentric satellite repeats represent possible candidates, which could play a role in this process. Indeed, in fission yeast and plants, heterochromatin formation and maintenance require complementary pericentric transcripts, which are processed to small RNAs that in turn guide heterochromatin formation and establishment of a transcriptionally silent state (Zaratiegui et al., 2007). While it remains to be determined whether a similar mechanism operates in mammals (Kanellopoulou et al., 2005; Murchison et al., 2005), numerous non-coding RNAs are expressed in a developmentally regulated manner (Ponting et al., 2009). Although some of these may be non-functional, others act in chromatin-dependent processes and silencing of large chromosomal domains during dosage compensation and genomic imprinting, e.g. Xist, Air and Kcnq1ot1 (Ponting et al., 2009; Wilusz et al., 2009). Others, like telomeric repeat-containing RNA (TERRA), are considered to regulate telomerase activity (Azzalin et al., 2007; Schoeftner and Blasco, 2008) or to facilitate heterochromatin formation at chromosome ends (Deng et al., 2009). Non-coding major satellite transcripts are of heterogenous length and contain repetitions of the 234bp-long AT-rich major satellite subunits (Lehnertz et al., 2003). Whether they correspond to transcriptional noise or have a specific function, how are they regulated and whether they harbor strand-specific properties have remained largely unanswered questions. Their expression has been related to proliferation and cell cycle state (Lu and Gilbert,

2007), yet they increase in quantity upon terminal differentiation of myoblasts (Terranova et al., 2005) and conflicting tissue specific expression patterns have been reported (Gaubatz and Cutler, 1990; Rudert et al., 1995; Schoeftner and Blasco, 2008). Here we set out to examine the expression status of both strands of pericentric major satellite repeats. We specifically investigated early cleavage stages of embryogenesis, as this is the time when important reorganization of pericentric domains takes place (Probst et al., 2007) and heterochromatin is established *de novo* at paternal major repeats.

We find that during early mouse development, major satellite repeats are highly expressed and subsequently rapidly downregulated. This event occurs precisely at the time when pericentric domains organize into chromocenters. Remarkably, we observed a strand–specific control of major satellite expression both spatially and temporally. This specific regulation not only corresponds to an intrinsic developmental program, but also reflects the characteristic parental epigenetic asymmetry. While blocking replication does not prevent the transcriptional upregulation of major satellites, chromocenter formation cannot be completed. Furthermore, interference with major transcripts following microinjection of LNA-DNA gapmers results in developmental arrest at the 2-cell stage before chromocenter formation. Based on these data we propose that the specific expression dynamics of major satellite repeats together with their strand-specific control represent necessary mechanisms during a critical time window in pre-implantation development that are of key importance to consolidate the maternal and to set up the paternal heterochromatic state at pericentric domains.

RESULTS

Transcriptional activation of major satellites followed by rapid downregulation coincides with chromocenter formation during early cleavage stages

To explore the dynamics of pericentric satellite expression during the first cleavage stages we carried out RNA FISH using nick-translation probes directed against major satellites. These predominant pericentric satellites are arranged in tandem repeats forming largely uninterrupted arrays and show little sequence deviation (Lehnertz et al., 2003; Vissel and Choo, 1989). While major satellite transcripts were barely detectable by RNA FISH in oocytes, we observed an increase in transcription in PN4/5 zygotes (Figure 1A, Table). Transcripts were predominantly paternal in agreement with the described higher transcriptional activity in the paternal pronucleus ((Aoki et al., 1997; Bouniol et al., 1995; Puschendorf et al., 2008), Table S1, S2). Interestingly, major satellite expression is dynamic during early cleavage stages: concomitant with the major zygotic gene activation (mZGA) (Nothias et al., 1995) we observed a burst in major satellite transcription at the 2-cell stage. Expression rapidly decreases and by the 8-cell stage only a few signals remained detectable. This transcriptional burst is absent if embryos are cultured in the presence of α-amanitin, indicating that major satellites are *de novo* transcribed (data not shown). Since transcription of major satellites can occur from both strands (Rudert et al., 1995), we decided to examine the expression of individual transcripts corresponding to each strand. Reverse transcription using strand-specific primers followed by PCR (Figure 1B) effectively revealed the presence of transcripts from both strands and confirmed the transcriptional burst of major satellites at the 2-cell stage revealed by RNA FISH.

Given the observed dynamics in major satellite expression we then investigated the organization of satellite repeats at the corresponding developmental stages and performed DNA FISH under conditions that preserve the 3D nuclear structure (Probst et al., 2007). We used probes specific for major satellites and telomeres to visualize nuclear organization (Figures 1C, D). For comparison, we carried out DNA FISH on mouse 3T3 fibroblasts, in which the organization of pericentric domains in chromocenter clusters has been carefully documented (Guenatri et al., 2004). As we had previously reported, pericentric domains restructure following fertilization from their gamete-specific organization to align around pro-nucleolar bodies in both parental pronuclei

of the zygote (Probst et al., 2007). The organization of pericentric chromatin into chromocenters takes place in the 2-cell embryo concomitant with the observed peak in expression: a clear transition in major satellite organization is detectable when comparing early versus late 2-cell embryos (Figure 1D). Ring structures are still present in embryos at 39h phCG, while most chromocenters are formed shortly before the second mitosis (48h phCG). We also noted that up to the 8-cell stage, interphase chromosomes in most nuclei adopt a Rabl configuration (Merico et al., 2007; Rabl, 1885) with centromeres on one side and the distal telomere on the opposite side of the nucleus. This configuration is lost at later developmental stages.

We conclude that major satellite sequences are *de novo* transcribed from the zygotic genome during pre-implantation development. Their transcription is dynamic and the transcriptional upregulation followed by a rapid downregulation coincides with the reorganization of pericentric satellites into chromocenters during a discrete time window at the 2-cell stage.

Strand-specific regulation of major satellite transcripts during early cleavage stages

In order to assess whether the expression of major satellites during early pre-implantation development is regulated in a strand-specific manner, we designed fluorescently labeled single-stranded oligonucleotide probes containing locked nucleic acid (LNA) bases (Figure 2A). We tested these strand-specific LNA-probes in 3T3 cells (Figure S1A) and then analyzed major satellite expression in zygotes, 2-cell, 4-cell and 8-cell embryos (Figure 2B). We chose 2-cell embryos at an early time point (39h phCG) corresponding to a late S/early G2 stage, and a stage just before cleavage (48h phCG), characterized by two distinct patterns of pericentric satellite organization (Figure 1D). In the paternal pronucleus of the zygote, we observed predominantly Reverse transcripts at the DAPI-bright rings corresponding to major satellites ((Probst et al., 2007), Table S3). Interestingly, a major peak of expression of the Forward transcripts was observed by 39h phCG (Figures 2B, S1B), while the Reverse strand was highly expressed in late 2-cell embryos showing a punctuate pattern similar to zygotes and 3T3 cells

(Figure 2E). By the 4-8 cell stages, only a few isolated Forward and Reverse transcripts were still detectable. Major satellite expression therefore decreases abruptly following the second cleavage. We found identical expression patterns in embryos flushed directly from the oviduct at the corresponding developmental stages, thereby excluding that the observed pattern is a consequence of culturing embryos *in vitro* (Figure S1C). Quantification of expression levels by strand-specific reverse transcription followed by Real-Time PCR analysis at the indicated developmental stages confirmed our RNA FISH observations (Figure 2F). At 39h phCG, the Forward transcripts have increased more than seventy fold compared to MII oocytes; this is followed by the upregulation of the Reverse transcripts by 48h phCG and a sharp downregulation of both Forward and Reverse transcripts at the 4-cell stage (Figures 2F, G). The decrease in Forward transcripts takes place progressively and is accompanied by an increase in Reverse transcript foci (Figure S1D), suggesting that the two transcripts co-exist within the same nucleus during the G2-phase of the 2-cell stage. Remarkably, and in contrast to somatic cells (Figure 2E), the Forward transcripts accumulate both at the DAPI-bright rings and in the cytoplasm, while the Reverse transcripts are retained in the nucleus (Figure 2A, S1B).

The distinct patterns observed for Forward and Reverse transcripts suggest that their dynamic is not merely a consequence of unscheduled expression of non-coding RNA at this developmental stage. We sought to confirm this by comparing major transcripts with the non-coding RNA transcribed from telomeric repeats (TERRA, (Azzalin et al., 2007; Schoeftner and Blasco, 2008)) and with polyA RNA. While TERRA transcripts are detectable in 2-cell embryos, they accumulate from the 4 and 8-cell stage on, when the expression of major satellites has reached low levels (Figure 2C). In most cases, we observed two bright sites of TERRA accumulation accompanied by small foci, which likely correspond to an accumulation of TERRA transcripts at the distal telomeres of sex chromosomes as described in ES cells (Zhang et al., 2009) and chromatin-associated transcripts at telomeres (Azzalin et al., 2007; Schoeftner and Blasco, 2008) respectively. To visualize Pol II transcriptional activity, we used an LNA probe directed

against the poly A tails of mRNA (Figure 2D). While in the zygote few signals are found in the nucleus, some transcripts are detected within the cytoplasm. At 39h phCG we observe prominent signals within the nucleus that could represent transcription factories (Iborra et al., 1996). Transcriptional activity, as judged from the amount of poly A RNA, is continuously increasing during the first cleavage stages (Figure 2D).

We conclude that during the first cell cycles major satellite transcripts exhibit expression patterns distinct from another non-coding RNA (TERRA) or general transcriptional activity (Figure 2F). They undergo a unique dynamic regulation with a burst in expression during which the two transcripts are regulated both spatially and temporally in a strand-specific manner.

Impact of cell cycle progression through S-phase on major satellite expression and chromocenter organization

To map the onset of satellite transcription at the 2-cell stage in relation to DNA replication, we combined immunostaining of the largest subunit (p150) of chromatin assembly factor 1 (CAF-1) as a marker for ongoing replication (Quivy et al., 2004) with RNA FISH for major satellites. During mitosis and shortly after cell division CAF-1 was not detectable (see also Figure S2A), but accumulated when embryos entered S-phase and marked replicating pericentric heterochromatin during mid/late S-phase (Figure 3A). Combined RNA FISH with CAF-1 immunostaining revealed that the major Forward transcripts progressively accumulate during S-phase.

Nucleosome disruption and restoration that occur during S-phase may entail changes in chromatin modifications (Probst et al., 2009). Importantly, during the earliest cleavage stages, the initially predominant H3.3 variant (van der Heijden et al., 2005) is progressively replaced by replicative histone H3 variants with different post-translational marks (Loyola et al., 2006) and following the active DNA demethylation of the paternal genome, both genomes undergo progressive passive demethylation (Reik et al., 2001). We therefore asked whether in 2-cell

embryos, replication and the accompanying changes in chromatin structure impact the expression dynamics of major satellites. For this, we blocked 2-cell embryos at the G1/S border with Aphidicolin, confirmed the absence of nucleotide incorporation and extracted RNA ~42h phCG when control embryos have reached the G2 stage (Figure 3B, C). Real-Time PCR quantification revealed about 2-fold less Forward and a slight increase in Reverse transcripts when embryos were cultured with Aphidicolin compared to DMSO (Figure 3D). The presence of only half the DNA content in Aphidicolin-treated embryos could explain the observed reduction in Forward transcript levels. However, the relative increase in Reverse transcripts suggests that the chromatin configuration in G1/S arrested embryos facilitates Reverse strand expression. Therefore, even though the Forward strand is transcribed during S-phase (Figure 3A), DNA replication and the linked changes in histone composition and DNA methylation do not significantly impact upon the burst of Forward transcripts, but may play a role in limiting Reverse strand expression.

We then asked whether the S-phase block affects the reorganization of pericentric domains. Indeed, while by 48h phCG, chromocenters had formed in most of the control embryos, in those embryos where S-phase was blocked, a fraction of the pericentric domains remained in the form of ring structures (Figure 3E).

We conclude that major Forward transcripts progressively accumulate during S-phase and that their upregulation follows an intrinsic developmental clock rather than being simply subject to cell-cycle control. Clearly, progression through S phase is required for chromocenter organization of a fraction of pericentric domains, indicating that transcriptional upregulation of Forward transcripts alone is not sufficient and suggesting a potential difference between maternal and paternal pericentric domains.

Parental-specific expression patterns of major satellites

In light of these results and the reported asymmetry in post-translational histone marks between the maternal and paternal pericentric domains (Probst et al., 2007; Puschendorf et al., 2008; Santos et al., 2005), we wondered whether major satellites are expressed in a parental-specific manner. Indeed, when analyzing the distribution of major satellite transcripts by RNA FISH we noted that they significantly localized to only half of the nucleus in 2-cell embryos. To distinguish maternal and paternal genomes we made use of the fact that at this stage only maternal chromatin carries the H3K9me3 mark and the two parental genomes are spatially segregated in some nuclei (Mayer et al., 2000b). We collected embryos at the early or late 2-cell stage and revealed H3K9me3 by immunostaining, followed by RNA FISH for Forward or Reverse transcripts, respectively (Figure 4A). Interestingly, in 15 out of 17 2-cell nuclei, in which we could observe a clear paternal/maternal separation, sites of Forward transcript accumulation were localized at paternal chromatin (Figure 4B, arrowhead). In contrast, the Reverse transcripts were not found to be limited to either genome (Figure 4C). Their localization to only half of the nucleus can be explained by the restriction of pericentric domains to one side in nuclei with Rabl configuration (Merico et al., 2007; Rabl, 1885) (Figure 1D).

Given that the Forward strand is predominantly expressed from paternal chromosomes at the 2-cell stage, we reasoned that its level should be reduced in parthenotes in which the complete genome is contributed by the oocyte and all pericentric domains carry somatic heterochromatin marks. We therefore generated diploid parthenotes and analyzed their satellite organization and transcription (Figure 5A, S3). Like in embryos, the pericentric satellites in 1-cell parthenotes organize in perinucleolar rings, which are resolved into chromocenters during the 2-cell stage (Figure 5B, C, S3). This argues for a developmental stage-specific organization of the pericentric domains that is initially independent of the parental origin and the corresponding epigenetic marks. As hypothesized, we found the levels of Forward transcripts to be reduced by approximately 6 fold in early 2-cell parthenotes compared to embryos (Figure 5B, C and D, S3 A). In agreement, the comparison of major transcript dynamics during early cleavage stages

between embryos and parthenotes clearly revealed the absence of a marked burst of Forward strand expression in parthenotes (Figure 5D). In contrast, we observed a peak of Reverse transcription in late 2-cell parthenotes; although 3 fold lower than in embryos (Figure 5C, D, S3A). The differences between parthenotes and embryos were specific to pericentric domains, as we did not find any significant difference in the amount, patterns or dynamics of TERRA RNA (Figure 5 B, C) or polyadenylated transcripts (Figure S3B) by RNA FISH.

Thus, these findings demonstrate the predominant paternal-specific major satellite expression, in particular of the Forward transcripts, which reflects the asymmetry between the two parental genomes and could be favored by the lack of somatic heterochromatic marks at the paternal pericentric domains.

Interference with major satellite transcription results in developmental arrest

To understand the importance of the transcription dynamics of major satellites for heterochromatin organization and embryonic development, we decided to interfere with their expression. Since RNA interference has been reported to operate during pre-implantation development (Svoboda et al., 2004), we first injected zygotes with either control siRNAs or siRNAs targeting major satellites. However, this had no impact on embryonic development or the organization of pericentric domains (Figure S4A), possibly because mainly the cytoplasmic Forward transcripts were targeted. Therefore we instead tried to deplete major RNA using LNA-DNA gapmers, which have previously been used to successfully interfere with nuclear transcripts (Mayer et al., 2006) and could deplete major transcripts in 3T3 cells despite their nuclear localization (data not shown). They are thought to lead to RNA degradation by activating the RNase H pathway (Rapozzi et al., 2006), however they may also interfere with the folding of RNA into secondary structures, the binding of proteins (Mayer et al., 2006) or transcription *per se* when designed with homology to a gene promoter (Beane et al., 2008). We therefore anticipated that LNA-DNA gapmers would affect the dynamics and function of major transcripts

in our system. We microinjected zygotes with either control LNA-DNA gapmers or a set of two gapmers specifically targeting Forward and Reverse major transcripts (Figure 6A, S4B) and confirmed the reduction in major transcript levels by qRT-PCR (Figure 6B). Injection of LNA gapmers targeting GFP or a control oligonucleotide had no significant impact on pre-implantation development. In contrast, embryos injected with LNA-DNA gapmers targeting major transcripts showed delayed development and/or developmental arrest at the 2-cell stage in a significantly elevated frequency compared to control injected embryos (Table 1). The arrested embryos could be maintained in culture for 4 days without obvious signs of degeneration/death (Figure S4C, I). In agreement with our qRT-PCR results, RNA-FISH revealed reduced levels of major transcripts, while global transcription was not affected (Figure S4C, II).

To narrow down the time of developmental arrest, we cultured microinjected embryos in the presence of BrdU to visualize nucleotide incorporation during DNA replication. In contrast to embryos, in which DNA replication was blocked with Aphidicolin, all microinjected embryos incorporated BrdU during the second cell cycle (Figure 6C, I). We can therefore exclude that the developmental arrest occurred prior to the second S-phase. Furthermore, absence of clear CAF-1 patterns in arrested and GFP-injected control embryos at 45h phCG suggests that the embryos are in G2 phase (Figure 6C, II), a critical developmental time window that corresponds to the peak in Reverse and the decline in Forward transcripts as well as the reorganization of pericentric heterochromatin into chromocenters (Figure 1D, S1D). To exclude that the arrest is a consequence of DNA damage or replication stress rather than a direct result of interference with major satellite transcripts, we used immunofluorescence staining for γH2AX. γH2AX is widely used as a marker for a response to DNA damage in eukaryotes (van Attikum and Gasser, 2009) and was found to be significantly increased in embryos treated with Aphidicolin (Figure 6C, III). In agreement with a previous study (Ziegler-Birling et al., 2009), we observed few γH2AX-enriched domains in embryos injected with LNA-DNA GFP gapmers as well as untreated *in vitro* cultured embryos (data not shown). No increase in H2AX phosphorylation was seen in embryos

injected with LNA-DNA gapmers targeting major satellite transcripts (Figure 6C, III). This argues against severe replication defects induced by the injection of LNA-DNA gapmers and/or the loss of major satellite transcripts.

To address the potential function of major satellite RNA, we explored the hypothesis that major transcripts, in a similar manner to Xist RNA on the inactive X-chromosome (Schoeftner et al., 2006), stabilize PRC1 complexes, which accumulate at paternal pericentric domains during the first cell cycles of embryonic development (Puschendorf et al., 2008). We therefore stained embryos injected with LNA-DNA gapmers targeting GFP or major satellites for Ring1b as a representative PRC1 component. We found however no significant difference in the distribution of Ring1b at maternal or paternal genomes or in its accumulation at the DAPI-bright pericentric domains compared to control (Figure 6D), suggesting that interference with major transcripts during the 2-cell stage does not delocalize PRC1 from paternal chromatin.

In order to evaluate the impact of depleting major satellite transcripts on the organization of pericentric heterochromatin, we fixed arrested embryos at 67h phCG for DNA FISH. While the GFP control-injected embryos cleaved to 4 or 8 cells revealing chromocenters, in embryos injected with gapmers directed against major transcripts part of the pericentric domains remained organized in ring structures (Figure 6E, compare to Figure 1D, early 2-cell embryos). Thus, interference with major satellite transcripts results in developmental arrest in the G2-phase of the 2-cell stage, before pericentric domains have completed their reorganization into chromocenters.

DISCUSSION

Unique strand-specific regulation of major satellite transcription during chromocenter formation at the 2-cell stage: activation followed by downregulation

In this study we provide the clear evidence for an exquisite strand-specific regulation of major satellite transcription during early cleavage stages when chromocenter formation occurs. A peak of expression immediately followed by downregulation takes place during this time window. The upregulation at the 2-cell stage, also observed for TERRA (Figure 2B) and other non-coding RNAs (Okamoto et al., 2004; Svoboda et al., 2004; Terranova et al., 2008), could relate to general changes at this developmental stage: (i) in chromatin, when H4 is hyperacetylated (Wiekowski et al., 1997) and DNA partially demethylated (Mayer et al., 2000a; Reik et al., 2001) and (ii) in the transcriptional machinery (Torres-Padilla and Tora, 2007). However, the abrupt downregulation of major satellites is unparalleled. The specific peak in transcription and the observed drop by the time that pericentric domains have organized into chromocenters suggests a link between chromocenter formation and these unique expression dynamics. Extensive changes in pericentric heterochromatin organization are also observed during reprogramming of primordial germ cells (Hajkova et al., 2008). Whether these changes are associated with specific expression dynamics of major satellites, and whether a common mechanism operates in different events of lineage reprogramming would be interesting to explore.

Remarkably, our qualitative analysis using RNA-FISH shows that major satellite transcripts exhibit unexpected strand-specific expression patterns and localization. While Forward transcripts accumulate during S-phase, Reverse strands are transcribed later, during G2 phase. Moreover, transcription of the Forward strand is strongly paternally biased and consequently reduced in parthenotes. Some aspects of the differential regulation of Forward and Reverse transcripts may be accounted for by the parental asymmetry (Puschendorf et al., 2008; Santos et al., 2005) and possibly by changes in DNA replication regulation (Hiratani et al., 2008). Investigating whether transcripts from the major satellites use specific promoters within the satellite repeats or are transcribed from interspersed transposons and require specific transcription factors should help to unravel their mode of regulation.

The subcellular distribution of the two complementary transcripts and the distinct response in their expression to a cell cycle block further support a strand-specific regulation. Reverse transcript signals are found in discrete nuclear foci at the DAPI-bright rings formed by the pericentric domains and may represent nascent transcription sites. Forward transcripts which coat a significant fraction of pericentric repeats (Figure S5) also localize to the cytoplasm indicating some export in early 2-cell embryos (Figure S1B). In embryos arrested at the G1/S border, the upregulation of Forward transcripts is not significantly affected and rather follows an intrinsic developmental program, as proposed for zygotic gene activation (Nothias et al., 1995). The Reverse transcription, which is activated later, is moderately increased in G1/S-arrested embryos and thereby parallels global transcription (Aoki et al., 1997). This increase compared to untreated embryos in G2 phase may be due to failure to establish a transcriptionally repressive state (Wiekowski et al., 1997). Intriguingly in these embryos, only a fraction of major satellite repeats, possibly corresponding to maternal pericentric repeats (Figure 1D), organizes into chromocenters. In contrast, paternal domains, which undergo more dramatic chromatin rearrangements and require a *de novo* formation of heterochromatin, would fail to do so.

Notably, following cleavage to the 4-cell stage, expression of major satellites from both strands drops abruptly in a concomitant fashion, likely implicating both transcriptional and post-transcriptional mechanisms. The general transcriptionally repressive state established during the course of the mZGA (Aoki et al., 1997; Schultz, 2002) and the global decrease in histone H4 acetylation (Wiekowski et al., 1997) can potentially contribute to the downregulation at the transcriptional level along with the higher order organization of pericentric repeats into chromocenters. At the same time, post-transcriptional regulation could come into place at the 4-cell stage as discussed later.

Thus, the exquisite transcriptional regulation specific to major satellite transcripts underlines a unique regulatory mechanism at a critical time window during development.

A functional role for the expression dynamics of major satellite transcripts

The developmental arrest observed following injection of LNA-DNA gapmers directed against major satellite transcripts strongly supports the functional relevance of these transcripts. Either the act of transcription and the associated chromatin remodeling or the transcripts as a structural component or through their processing could be important. Indeed, the rapid disappearance of major satellite transcripts by the 4-cell stage implies both transcriptional and post-transcriptional processing. In analogy to RNAi-mediated degradation and RNA-directed transcriptional silencing mechanisms in *S. pombe* (White and Allshire, 2008), it is tempting to speculate that either major transcripts could fold into partially double-stranded secondary structures (Djupedal et al., 2009) or that the two complementary transcripts hybridize to double-stranded intermediates, which are further processed to trigger heterochromatin formation at the paternal domains. Given that RNA interference operates in oocytes (Watanabe et al., 2008) and pre-implantation embryos, where it is involved in transposon control (Svoboda et al., 2004; Watanabe et al., 2008), this is an attractive possibility. The expression kinetics of Forward and Reverse transcripts (Figure S1D) and the observation that double stranded major RNA can rescue the developmental arrest of embryos expressing a K27R mutated form of H3.3 (Santenard et al.) are compatible with such a scenario. However, to determine whether small dsRNAs corresponding to major satellite transcripts accumulate at the 2-cell stage, a detailed analysis including deep sequencing of small RNA libraries derived from the corresponding developmental stages would be necessary. Alternatively mechanisms independent of RNAi, as found in *S. cerevisae,* during which antisense transcripts act in *cis* or in *trans* on homologous target sequences to induce transcriptional silencing (Camblong et al., 2009), can also be envisaged. Future studies should elucidate the pathways involved in degradation as well as the possible interaction with mechanisms operating at the transcriptional level that together result in the low constitutive expression level at later developmental stages.

Interestingly, interference by LNA-DNA gapmers can not only lead to RNA degradation, but also inhibit RNA folding or RNA–protein interaction as shown for the binding of the nucleolar remodeling complex (NoRC) to short intergenic RNA molecules covering the rDNA promoter (Mayer et al., 2006), thus affecting their functional role. In this case, LNA-DNA gapmers were readily effective in interfering with RNA-mediated stabilization of the NoRC complex and with the formation of heterochromatin at the rDNA locus. A similar structural role for major transcripts could be envisaged in stabilizing the PRC1 complexes that accumulate at paternal pericentric domains in an Ezh2 and H3K27me3 independent manner (Puschendorf et al., 2008). However, we have not found evidence that interference with major transcripts during the 2-cell stage delocalizes PRC1 from paternal chromatin. Alternatively, major transcripts could be involved in stabilizing heterochromatin components at maternal and/or in their local recruitment to paternal domains. Potential candidates are histone methyltransferases and HP1. HP1 has RNA-binding capacity (Maison et al., 2002; Muchardt et al., 2002) and interacts in a post-translationally modified form specifically with major Forward transcripts (Maison et al., submitted). At paternal domains, recruitment of HP1 in combination with an active histone methyltransferase could lead during the next cell cycles to accumulation of H3K9me3 and HP1 that could further spread in the absence of major transcripts using a self-perpetuating loop (Maison and Almouzni, 2004) and progressively displace PRC1 components. Our observation of a partial co-localization between Forward transcripts and HP1β (Figure S5) together with the fact that exogenously expressed major transcripts can lead to reduced HP1 at chromocenters (Frescas et al., 2008) would be consistent with this scenario. We propose that the combined expression dynamics of Forward and Reverse major satellite transcripts play an important role in setting up the paternal intermediate heterochromatin state and consolidating the maternal ones to enable proper cell division.

Taken together, we have highlighted a unique strand-specific regulation of major satellite repeats during mouse pre-implantation development. The expression of major satellites as well as the major change in their subnuclear higher-order organization illustrates the extremely dynamic and deliberate changes that occur during this critical time window when maternal pericentric heterochromatin is reorganized and the paternal one is set up for subsequent development.

EXPERIMENTAL PROCEDURES

Antibodies and LNA oligonucleotide probes

We used the following antibodies for Immunofluorescence staining: anti-CAF1 (p150, (Quivy et al., 2004), 1:500-1:800), anti-H3K9me3 (Upstate, 1:200), anti-Ring1B (MBL, 1:200), anti-γH2AX (Millipore, 1:500) and anti-BrdU (Harlan Seralab, 1:800) in combination with cross-absorbed Alexa 488, 594 or 647-coupled secondary antibodies (Molecular Probes).

We obtained fluorescently labeled LNA oligonucleotide probes and LNA-DNA gapmers from Exiqon and Sigma Proligo (Table S4).

Mouse embryo collection and culture

Superovulated F1 (C57BL/6 x DBA) females (Charles River) were mated with B6D2F1 males and embryos were either flushed from the oviduct at the desired developmental stage or isolated from the ampullae as zygotes and cultivated in microdrops of M16 medium (Sigma) at 37°C under 5% CO_2. To block replication we supplemented M16 medium with 2.5μg/mL Aphidicolin (Sigma).

To generate diploid parthenotes, we isolated MII oocytes 16 h phCG and activated them in Ca^{2+} - free M16 medium containing 10mM $SrCl_2$ for 1h followed by 6h in M16 medium containing 5μg/mL Cytochalasin B.

Microinjection

We isolated zygotes from superovulated mated B6D2F1 females ~20h phCG and microinjected ~ 10pL LNA gapmers (10μM) diluted in 6mM HEPES-pH 7.5, 20mM KCl, 0.2mM $MgCl_2$ into the cytoplasm between 24-28h phCG using an Eppendorf Micromanipulator on a Nikon inverted microscope.

Immunofluorescence staining and RNA FISH

Oocytes and embryos were prepared for Immunofluorescence, RNA FISH and Immuno-RNA FISH as described (Okamoto et al., 2004; Terranova et al., 2008), except that we carried out hybridization with fluorescently labeled LNA probes (0.4μM, Exiqon) in 50% Formamide (Sigma), 2x SSC (Sigma), 10% Dextran Sulfate (Fluka), 10mM VRC and 2mg/mL BSA (NEB) for 35min at 37°C and washed in 0.1x SSC at 60°C. DNA FISH on cells and embryos was performed as depicted (Guenatri et al., 2004; Probst et al., 2007), except that the hybridization mix contained LNA probes (0.1μM) and post-hybridization washes were in 0.1x SSC at 60°C. To reveal BrdU, DNA was denatured as for DNA FISH before immunostaining.

Microscope analysis and Image processing

We acquired brightfield images of embryos and cells under a Nikon inverted microscope eclipse TS100 equipped with a Digital Sight camera system (Nikon), and fluorescent images using the Deltavision real-time (RT) microscope (Applied Precision; 40x, numerical aperture (NA) of 1.35, 63x and 100x objectives with a NA of 1.4). We deconvolved images with SoftWorx and used

Adobe Photoshop CS3 and ImageJ for further processing. If not stated otherwise maximum intensity projections are shown.

RNA preparation and RT-PCR analysis

After addition of 0.5pg of an *in vitro* transcribed exogenous standard per cell in the embryo, RNA (Trizol, Invitrogen) from at least 10 embryos was Dnase I (Sigma) treated, reverse transcribed (Superscript II, Invitrogen) with strand specific primers (Lehnertz et al., 2003) and major transcript levels were quantified by Real-Time PCR (Terranova et al., 2005).

REFERENCES

Aoki, F., Worrad, D.M., and Schultz, R.M. (1997). Regulation of transcriptional activity during the first and second cell cycles in the preimplantation mouse embryo. Dev Biol *181*, 296-307.

Azzalin, C.M., Reichenbach, P., Khoriauli, L., Giulotto, E., and Lingner, J. (2007). Telomeric repeat containing RNA and RNA surveillance factors at mammalian chromosome ends. Science *318*, 798-801.

Beane, R., Gabillet, S., Montaillier, C., Arar, K., and Corey, D.R. (2008). Recognition of chromosomal DNA inside cells by locked nucleic acids. Biochemistry *47*, 13147-13149.

Bouniol, C., Nguyen, E., and Debey, P. (1995). Endogenous transcription occurs at the 1-cell stage in the mouse embryo. Exp Cell Res *218*, 57-62.

Brown, S.W. (1966). Heterochromatin. Science *151*, 417-425.

Camblong, J., Beyrouthy, N., Guffanti, E., Schlaepfer, G., Steinmetz, L.M., and Stutz, F. (2009). Trans-acting antisense RNAs mediate transcriptional gene cosuppression in S. cerevisiae. Genes Dev *23*, 1534-1545.

Deng, Z., Norseen, J., Wiedmer, A., Riethman, H., and Lieberman, P.M. (2009). TERRA RNA binding to TRF2 facilitates heterochromatin formation and ORC recruitment at telomeres. Mol Cell *35*, 403-413.

Djupedal, I., Kos-Braun, I.C., Mosher, R.A., Soderholm, N., Simmer, F., Hardcastle, T.J., Fender, A., Heidrich, N., Kagansky, A., Bayne, E.*, et al.* (2009). Analysis of small RNA in fission yeast; centromeric siRNAs are potentially generated through a structured RNA. Embo J.

Fraser, P., and Bickmore, W. (2007). Nuclear organization of the genome and the potential for gene regulation. Nature *447*, 413-417.

Frescas, D., Guardavaccaro, D., Kuchay, S.M., Kato, H., Poleshko, A., Basrur, V., Elenitoba-Johnson, K.S., Katz, R.A., and Pagano, M. (2008). KDM2A represses transcription of centromeric satellite repeats and maintains the heterochromatic state. Cell Cycle *7*, 3539-3547.

Gaubatz, J.W., and Cutler, R.G. (1990). Mouse satellite DNA is transcribed in senescent cardiac muscle. J Biol Chem *265*, 17753-17758.

Guenatri, M., Bailly, D., Maison, C., and Almouzni, G. (2004). Mouse centric and pericentric satellite repeats form distinct functional heterochromatin. J Cell Biol *166*, 493-505.

Hajkova, P., Ancelin, K., Waldmann, T., Lacoste, N., Lange, U.C., Cesari, F., Lee, C., Almouzni, G., Schneider, R., and Surani, M.A. (2008). Chromatin dynamics during epigenetic reprogramming in the mouse germ line. Nature *452*, 877-881.

Hemberger, M., Dean, W., and Reik, W. (2009). Epigenetic dynamics of stem cells and cell lineage commitment: digging Waddington's canal. Nat Rev Mol Cell Biol *10*, 526-537.

Hiratani, I., Ryba, T., Itoh, M., Yokochi, T., Schwaiger, M., Chang, C.W., Lyou, Y., Townes, T.M., Schubeler, D., and Gilbert, D.M. (2008). Global reorganization of replication domains during embryonic stem cell differentiation. PLoS Biol *6*, e245.

Iborra, F.J., Pombo, A., Jackson, D.A., and Cook, P.R. (1996). Active RNA polymerases are localized within discrete transcription "factories' in human nuclei. J Cell Sci *109 (Pt 6)*, 1427-1436.

Kanellopoulou, C., Muljo, S.A., Kung, A.L., Ganesan, S., Drapkin, R., Jenuwein, T., Livingston, D.M., and Rajewsky, K. (2005). Dicer-deficient mouse embryonic stem cells are defective in differentiation and centromeric silencing. Genes Dev *19*, 489-501.

Lehnertz, B., Ueda, Y., Derijck, A.A., Braunschweig, U., Perez-Burgos, L., Kubicek, S., Chen, T., Li, E., Jenuwein, T., and Peters, A.H. (2003). Suv39h-mediated histone H3 lysine 9 methylation directs DNA methylation to major satellite repeats at pericentric heterochromatin. Curr Biol *13*, 1192-1200.

Loyola, A., Bonaldi, T., Roche, D., Imhof, A., and Almouzni, G. (2006). PTMs on H3 variants before chromatin assembly potentiate their final epigenetic state. Mol Cell *24*, 309-316.

Lu, J., and Gilbert, D.M. (2007). Proliferation-dependent and cell cycle regulated transcription of mouse pericentric heterochromatin. J Cell Biol *179*, 411-421.

Maison, C., and Almouzni, G. (2004). HP1 and the dynamics of heterochromatin maintenance. Nat Rev Mol Cell Biol *5*, 296-304.

Maison, C., Bailly, D., Peters, A.H., Quivy, J.P., Roche, D., Taddei, A., Lachner, M., Jenuwein, T., and Almouzni, G. (2002). Higher-order structure in pericentric heterochromatin involves a distinct pattern of histone modification and an RNA component. Nat Genet *30*, 329-334.

Mayer, C., Schmitz, K.M., Li, J., Grummt, I., and Santoro, R. (2006). Intergenic transcripts regulate the epigenetic state of rRNA genes. Mol Cell *22*, 351-361.

Mayer, W., Niveleau, A., Walter, J., Fundele, R., and Haaf, T. (2000a). Demethylation of the zygotic paternal genome. Nature *403*, 501-502.

Mayer, W., Smith, A., Fundele, R., and Haaf, T. (2000b). Spatial separation of parental genomes in preimplantation mouse embryos. J Cell Biol *148*, 629-634.

Merico, V., Barbieri, J., Zuccotti, M., Joffe, B., Cremer, T., Redi, C.A., Solovei, I., and Garagna, S. (2007). Epigenomic differentiation in mouse preimplantation nuclei of biparental, parthenote and cloned embryos. Chromosome Res.

Muchardt, C., Guilleme, M., Seeler, J.S., Trouche, D., Dejean, A., and Yaniv, M. (2002). Coordinated methyl and RNA binding is required for heterochromatin localization of mammalian HP1alpha. EMBO Rep *3*, 975-981.

Murchison, E.P., Partridge, J.F., Tam, O.H., Cheloufi, S., and Hannon, G.J. (2005). Characterization of Dicer-deficient murine embryonic stem cells. Proc Natl Acad Sci U S A *102*, 12135-12140.

Nothias, J.Y., Majumder, S., Kaneko, K.J., and DePamphilis, M.L. (1995). Regulation of gene expression at the beginning of mammalian development. J Biol Chem *270*, 22077-22080.

Okamoto, I., Otte, A.P., Allis, C.D., Reinberg, D., and Heard, E. (2004). Epigenetic dynamics of imprinted X inactivation during early mouse development. Science *303*, 644-649.

Ponting, C.P., Oliver, P.L., and Reik, W. (2009). Evolution and functions of long noncoding RNAs. Cell *136*, 629-641.

Probst, A.V., Dunleavy, E., and Almouzni, G. (2009). Epigenetic inheritance during the cell cycle. Nat Rev Mol Cell Biol *10*, 192-206.

Probst, A.V., Santos, F., Reik, W., Almouzni, G., and Dean, W. (2007). Structural differences in centromeric heterochromatin are spatially reconciled on fertilisation in the mouse zygote. Chromosoma *116*, 403-415.

Puschendorf, M., Terranova, R., Boutsma, E., Mao, X., Isono, K., Brykczynska, U., Kolb, C., Otte, A.P., Koseki, H., Orkin, S.H.*, et al.* (2008). PRC1 and Suv39h specify parental asymmetry at constitutive heterochromatin in early mouse embryos. Nat Genet *40*, 411-420.

Quivy, J.P., Roche, D., Kirschner, D., Tagami, H., Nakatani, Y., and Almouzni, G. (2004). A CAF-1 dependent pool of HP1 during heterochromatin duplication. Embo J *23*, 3516-3526.

Rabl, C. (1885). Über Zellteilung. Morph Jb *10*, 214-311.

Rapozzi, V., Cogoi, S., and Xodo, L.E. (2006). Antisense locked nucleic acids efficiently suppress BCR/ABL and induce cell growth decline and apoptosis in leukemic cells. Mol Cancer Ther *5*, 1683-1692.

Reik, W., Dean, W., and Walter, J. (2001). Epigenetic reprogramming in mammalian development. Science *293*, 1089-1093.

Rudert, F., Bronner, S., Garnier, J.M., and Dolle, P. (1995). Transcripts from opposite strands of gamma satellite DNA are differentially expressed during mouse development. Mamm Genome *6*, 76-83.

Santenard, A., Ziegler-Birling, C., Koch, M., Tora, L., Bannister, A.J., and Torres-Padilla, M.E. Heterochromatin formation in the mouse embryo requires critical residues of the histone variant H3.3. Nat Cell Biol.

Santos, F., Peters, A.H., Otte, A.P., Reik, W., and Dean, W. (2005). Dynamic chromatin modifications characterise the first cell cycle in mouse embryos. Dev Biol *280*, 225-236.

Schoeftner, S., and Blasco, M.A. (2008). Developmentally regulated transcription of mammalian telomeres by DNA-dependent RNA polymerase II. Nat Cell Biol *10*, 228-236.

Schoeftner, S., Sengupta, A.K., Kubicek, S., Mechtler, K., Spahn, L., Koseki, H., Jenuwein, T., and Wutz, A. (2006). Recruitment of PRC1 function at the initiation of X inactivation independent of PRC2 and silencing. Embo J *25*, 3110-3122.

Schultz, R.M. (2002). The molecular foundations of the maternal to zygotic transition in the preimplantation embryo. Hum Reprod Update *8*, 323-331.

Solovei, I., Kreysing, M., Lanctot, C., Kosem, S., Peichl, L., Cremer, T., Guck, J., and Joffe, B. (2009). Nuclear architecture of rod photoreceptor cells adapts to vision in mammalian evolution. Cell *137*, 356-368.

Surani, M.A. (2001). Reprogramming of genome function through epigenetic inheritance. Nature *414*, 122-128.

Svoboda, P., Stein, P., Anger, M., Bernstein, E., Hannon, G.J., and Schultz, R.M. (2004). RNAi and expression of retrotransposons MuERV-L and IAP in preimplantation mouse embryos. Dev Biol *269*, 276-285.

Terranova, R., Sauer, S., Merkenschlager, M., and Fisher, A.G. (2005). The reorganisation of constitutive heterochromatin in differentiating muscle requires HDAC activity. Exp Cell Res *310*, 344-356.

Terranova, R., Yokobayashi, S., Stadler, M.B., Otte, A.P., van Lohuizen, M., Orkin, S.H., and Peters, A.H. (2008). Polycomb group proteins Ezh2 and Rnf2 direct genomic contraction and imprinted repression in early mouse embryos. Dev Cell *15*, 668-679.

Torres-Padilla, M.E., and Tora, L. (2007). TBP homologues in embryo transcription: who does what? EMBO Rep *8*, 1016-1018.

van Attikum, H., and Gasser, S.M. (2009). Crosstalk between histone modifications during the DNA damage response. Trends Cell Biol *19*, 207-217.

van der Heijden, G.W., Dieker, J.W., Derijck, A.A., Muller, S., Berden, J.H., Braat, D.D., van der Vlag, J., and de Boer, P. (2005). Asymmetry in histone H3 variants and lysine methylation between paternal and maternal chromatin of the early mouse zygote. Mech Dev *122*, 1008-1022.

Vissel, B., and Choo, K.H. (1989). Mouse major (gamma) satellite DNA is highly conserved and organized into extremely long tandem arrays: implications for recombination between nonhomologous chromosomes. Genomics *5*, 407-414.

Watanabe, T., Totoki, Y., Toyoda, A., Kaneda, M., Kuramochi-Miyagawa, S., Obata, Y., Chiba, H., Kohara, Y., Kono, T., Nakano, T.*, et al.* (2008). Endogenous siRNAs from naturally formed dsRNAs regulate transcripts in mouse oocytes. Nature *453*, 539-543.

White, S.A., and Allshire, R.C. (2008). RNAi-mediated chromatin silencing in fission yeast. Curr Top Microbiol Immunol *320*, 157-183.

Wiekowski, M., Miranda, M., Nothias, J.Y., and DePamphilis, M.L. (1997). Changes in histone synthesis and modification at the beginning of mouse development correlate with the establishment of chromatin mediated repression of transcription. J Cell Sci *110 (Pt 10)*, 1147-1158.

Wilusz, J.E., Sunwoo, H., and Spector, D.L. (2009). Long noncoding RNAs: functional surprises from the RNA world. Genes Dev *23*, 1494-1504.

Worrad, D.M., Ram, P.T., and Schultz, R.M. (1994). Regulation of gene expression in the mouse oocyte and early preimplantation embryo: developmental changes in Sp1 and TATA box-binding protein, TBP. Development *120*, 2347-2357.

Zaratiegui, M., Irvine, D.V., and Martienssen, R.A. (2007). Noncoding RNAs and gene silencing. Cell *128*, 763-776.

Zhang, L.F., Ogawa, Y., Ahn, J.Y., Namekawa, S.H., Silva, S.S., and Lee, J.T. (2009). Telomeric RNAs Mark Sex Chromosomes in Stem Cells. Genetics *182*, 685-698.

Ziegler-Birling, C., Helmrich, A., Tora, L., and Torres-Padilla, M.E. (2009). Distribution of p53 binding protein 1 (53BP1) and phosphorylated H2A.X during mouse preimplantation development in the absence of DNA damage. Int J Dev Biol *53*, 1003-1011.

ACKNOWLEDGMENTS

We thank S. Jannet and I. Grandjean at the Curie animal facility, the Curie PITC-IBiSA@pasteur imaging facility, C. Escude for discussion on LNA technology, A. Londono-Vallejo for the telomere probes and E. Heard and A. Cook for critical reading. This work and A.V.P were supported by ANR ‘‘CenRNA’’ NT05-4_42267 and ANR ‘‘FaRC’’ PCV06_142302, la Ligue Nationale contre le Cancer (Equipe labellisée la Ligue), EMBO, Swiss National Fund (SNF), PIC Programs (‘‘Retinoblastome and ‘‘Replication, Instabilité chromosomique et cancer’’), the European Commission Network of Excellence Epigenome (LSHG-CT-2004-503433), ACI-2007-Cancéropôle IdF ‘‘Breast cancer and Epigenetics.

FIGURES LEGENDS

Figure 1: Major satellite repeats undergo dynamic changes in expression concomitant with structural rearrangements during pre-implantation development.

(A) RNA FISH using a nick translation probe for major satellites (red). Percentage of analyzed embryos (n) with no, less than 30 or more than 30 RNA FISH signals are shown in the table below. (B) Strand specific RT-PCR of major transcripts normalized to an exogenous standard. (C) Schematic representation of a typical mouse acrocentric chromosome. (D) Bright field and fluorescence images of cells and embryos at different developmental stages, for which major satellites (red) and telomeres (green) have been revealed by DNA FISH. DNA is counterstained with DAPI (grey). Scale bar, 10 μm. PB, polar body.

Figure 2: Major satellite transcripts show strand-specific expression patterns

(A) Scheme of fluorescently labeled LNA probes designed to specifically reveal Forward (1,3) and Reverse (2,4) transcripts of major satellites. (B) Major transcripts detected by strand-specific LNA probes: Forward (green) and Reverse (red). (C) Co-detection of major transcripts (green) with telomeric repeat-containing RNA (TERRA) (red). (D) Co-detection of major transcripts (red) with bulk poly-adenylated RNA (green). Enlargements show the paternal pronuclei of the zygote and representative nuclei for the other cleavage stages. (E) RNA FISH for major satellites in 3T3 cells. DNA is counterstained with DAPI (grey). Scale bar, 10μm. PB, polar body. (F) Reverse transcription with strand-specific primers followed by quantification of major transcripts relative to an exogenous standard using Real-Time PCR. Mean fold changes +/- SD of transcript levels relative to MII oocytes (set to 1) are shown. (G) Schematic representation of expression patterns of the analyzed transcripts from zygotes to 8-cell embryos (see also Figure S1).

Figure 3: The burst of major satellite expression is independent of progression through S-phase

(A) At different time points following hCG injection embryos were stained for p150 CAF-1 (red) followed by RNA FISH for Forward transcripts (green). (B) After completion of the first S-phase, embryos were cultured with and without BrdU and in the presence of Aphidicolin to block DNA replication in the second S-phase and collected together with mock treated embryos at 42h phCG for RNA extraction and BrdU staining and at 48h phCG for DNA FISH. (C) Incorporated BrdU (red) in 2-cell embryos cultured with or without Aphidicolin. (D) RealTime PCR quantification of major transcripts after strand-specific reverse transcription. Mean fold changes +/- SD of transcript levels in Aphidicolin relative to DMSO- treated embryos (set to 1) are shown. (E) DNA FISH for major satellites (red) and telomeres (green). Arrowheads point to pericentric domains organized as chromocenters or ring-structures, respectively (see also Figure S2). DNA is counterstained with DAPI (grey). Scale bar, 10μm. PB, polar body.

Figure 4: Major satellite transcripts show parental asymmetry

(A) 2-cell embryos were fixed at 39h phCG (B) and 48h phCG (C) and processed for immunostaining followed by RNA FISH. (B-C) Representative 2-cell embryos stained for H3K9me3 (red in B and green in C) followed by RNA FISH for Forward (green, B) or Reverse transcripts (red, C). DNA is counterstained with DAPI (grey). Scale bar, 10μm. PB, polar body.

Figure 5: The peak of Forward strand expression is absent in 2-cell parthenogenetic embryos

(A) 2-cell embryos and parthenotes were collected for RNA extraction and RNA FISH at ~ 27h and ~38h post-fertilization (pf) or post-activation (pa) respectively. (B, C) RNA FISH for Forward (green) and Reverse (red) transcripts in representative 2-cell embryos and parthenotes fixed at ~ 27h (B) and ~38h (C) pf or pa respectively. For both time points mean fold changes +/- SD of transcript levels in parthenotes relative to embryos (set to 1) as determined by qRT-PCR are shown. Early and late 2-cell embryos and parthenotes were also processed for TERRA (red)

RNA FISH and DNA FISH with probes revealing major satellites (red) and telomeres (green). DNA is counterstained with DAPI (grey). Scale bar, 10μm. PB, polar body. (D) Dynamics of major satellite expression in embryos and parthenotes. Reverse transcription with strand-specific primers followed by quantification of major transcripts relative to an exogenous standard using Real-Time PCR. Mean fold changes +/- SD of transcript levels in embryos (colored lines) and parthenotes (bars) relative to the amount of transcripts in MII oocytes (set to 1) are shown (see also Figure S3).

Figure 6: Depletion of major satellite transcripts leads to developmental arrest before chromocenter formation is completed

(A) Zygotes were injected between 24-27h phCG with LNA-DNA gapmers directed against GFP, control LNA-DNA gapmers or with either set of two LNA-DNA gapmers directed against the Forward and Reverse major transcripts. Embryos were collected for RNA extraction, RNA FISH and BrdU staining at 42h, for Immunostaining at 45h and for DNA FISH at 67h phCG. (B) Real-time PCR quantification of major transcripts after strand-specific reverse transcription. Mean transcript levels +/- SD in 2-cell embryos injected with LNA-DNA gapmers 1+2 compared to GFP (set to 1) from two independent microinjections are shown. (C) I. BrdU incorporation (red) in 2-cell embryos microinjected with LNA DNA-gapmers GFP or major 1+2 and in Aphidicolin-treated embryos as negative control. II. Immunostaining of microinjected embryos for the largest subunit of the CAF-1 complex (p150, red) as S-phase marker compared to 2-cell embryos in S-phase. III. γH2AX staining (green) in microinjected embryos compared to Aphidicolin-treated embryos. (D) Microinjected 2-cell embryos stained for Ring1B (green) and H3K9me3 (red). (E) Right panels show brightfield images of microinjected embryos 72h phCG. Middle and left panels represent embryos stained by DNA FISH for major satellites (red) and telomeres (green) (see also Figure S4). DNA was counterstained with DAPI (grey). Scale bar, 10μm. PB, polar body.

Table 1: Developmental phenotype of embryos microinjected with LNA-DNA gapmers

59 779 characters

Figure 1

A RNA FISH:
DAPI major satellites

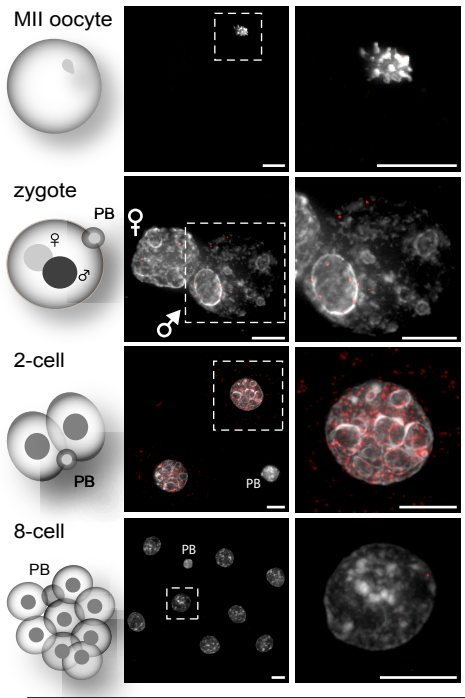

developmental stage	% of embryos with RNA FISH signals 0	< 30	>30	no
MII oocyte	82	18	-	22
Zygote	23.5	76.5	-	17
2-cell	-	-	100*	15
8-cell	14	86	-	14

* most embryos show > 200 signals

B Reverse Transcription

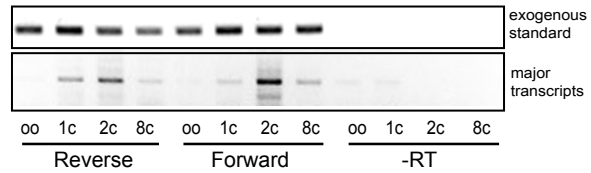

C Typical mouse acrocentric chromosome

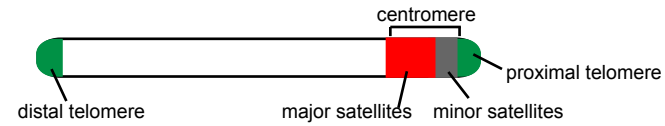

D DNA FISH: DAPI major satellites telomeres

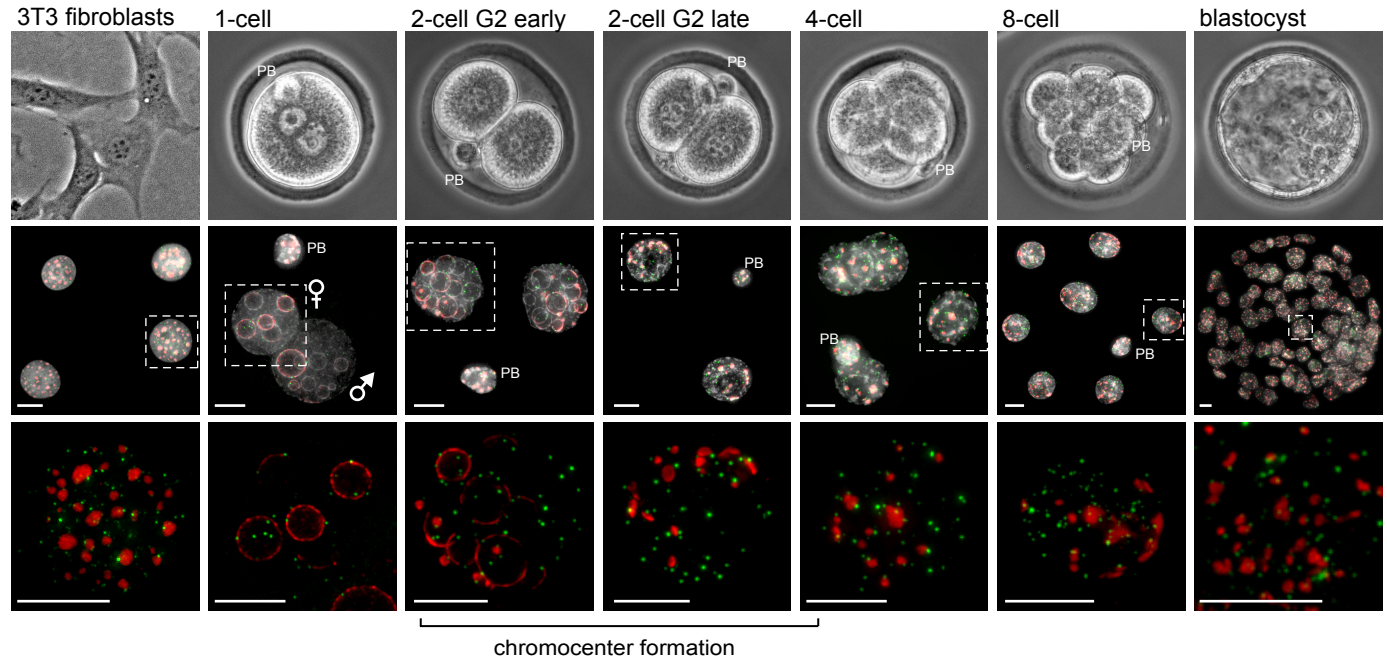

Figure 2

A Strand specific LNA probes for major satellite transcripts

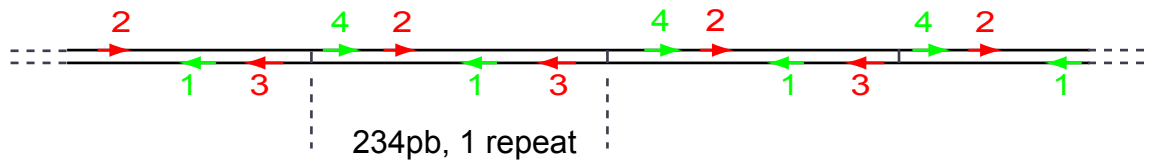

RNA FISH

B DAPI majorForward majorReverse

C DAPI major F+R TERRA

D DAPI polyA majorF+R

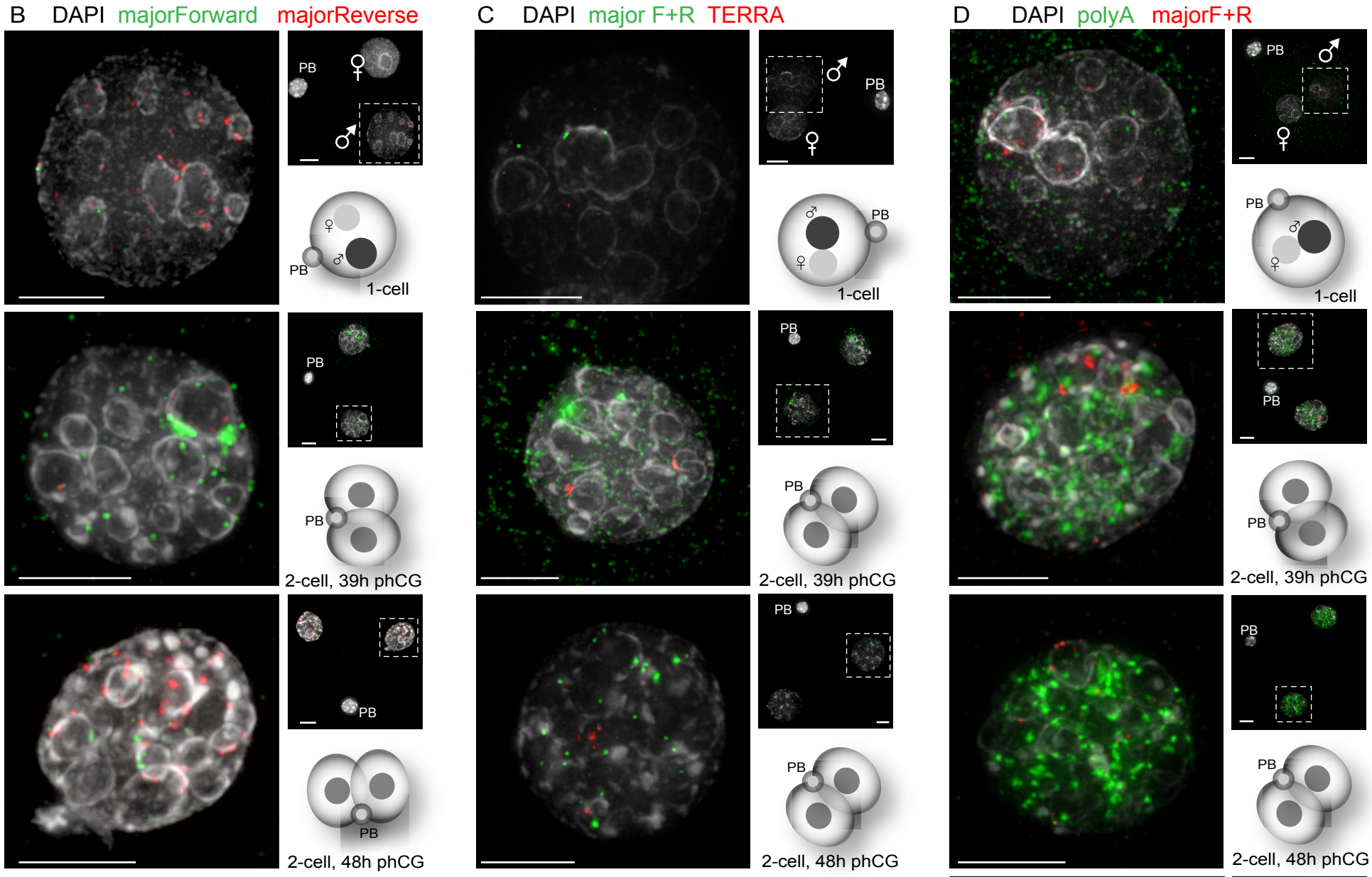

E RNA FISH
DAPI majorForward majorReverse

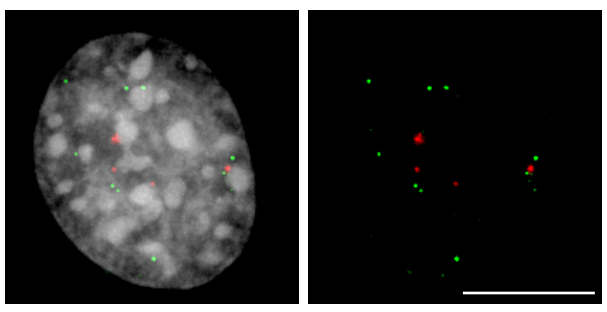

F Real-Time PCR quantification

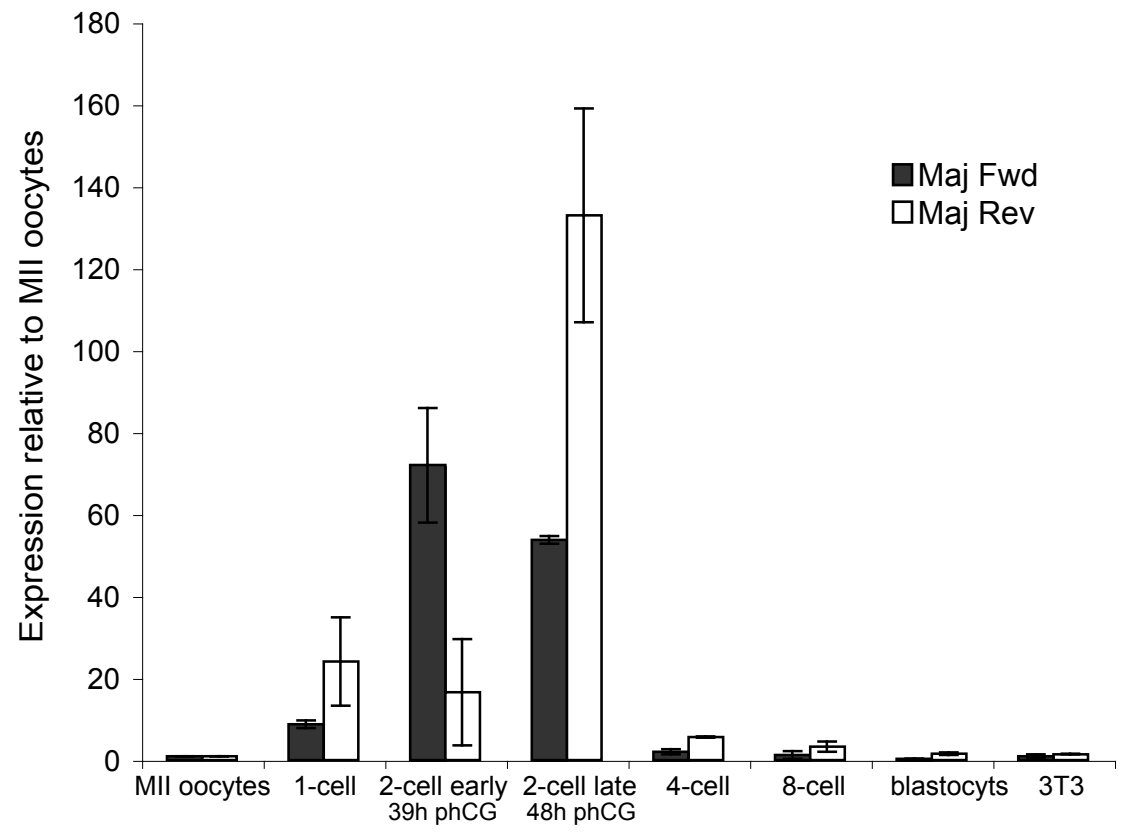

G Schematic representation of expression patterns

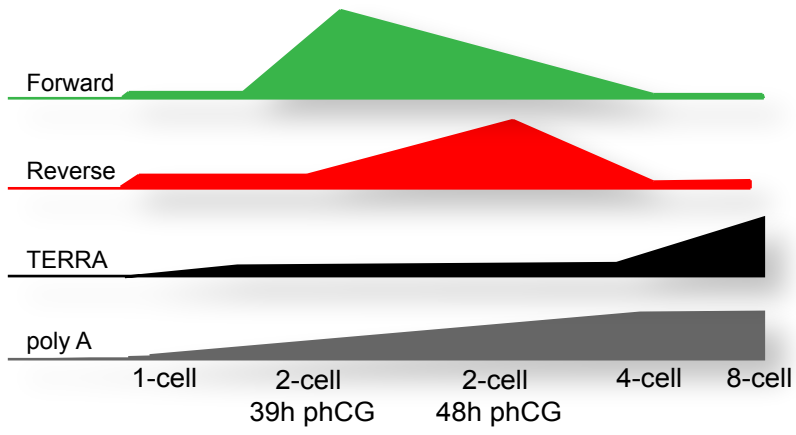

Figure 3

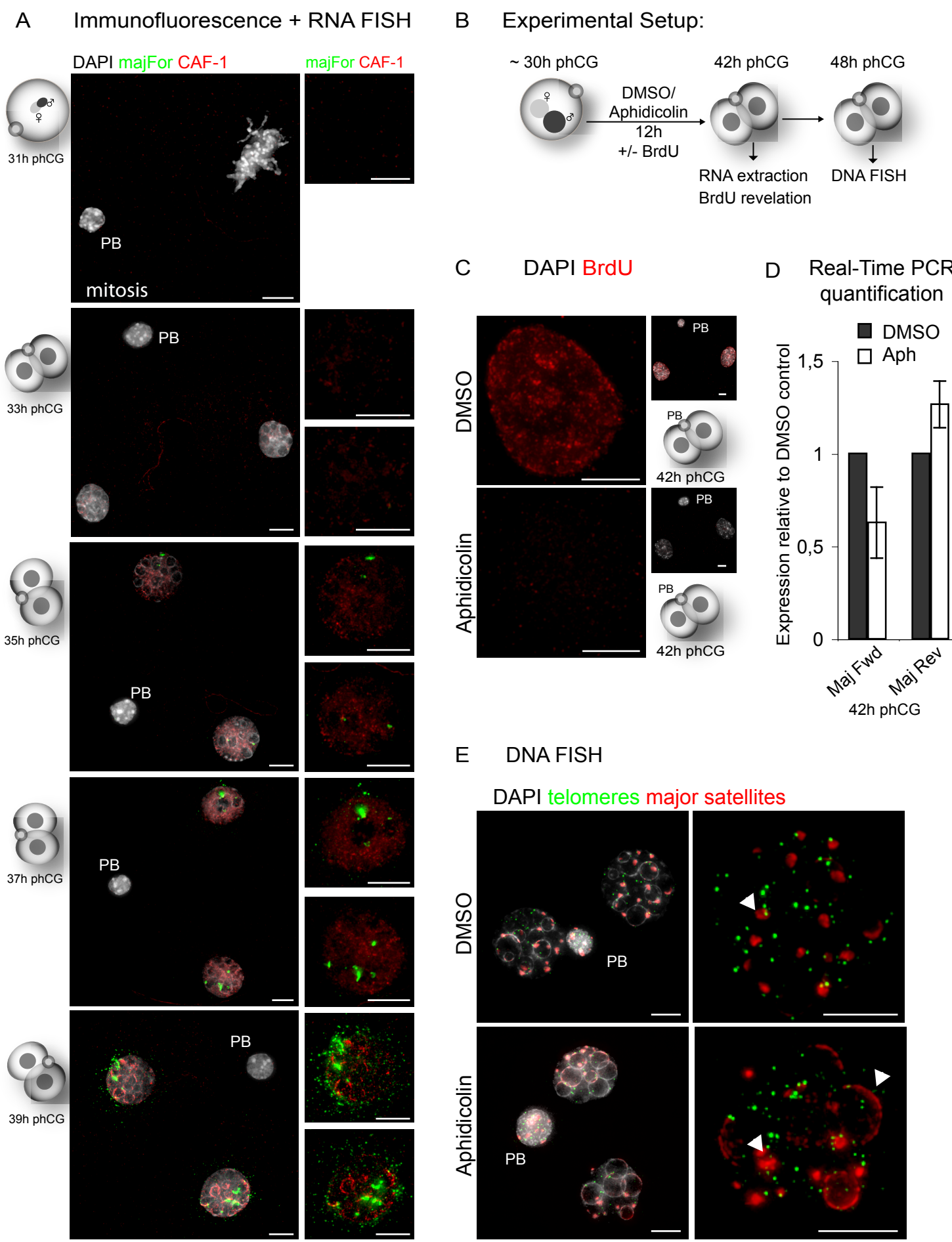
A
Immunofluorescence + RNA FISH
DAPI majFor CAF-1
majFor CAF-1
31h phCG
PB
mitosis
33h phCG
PB
35h phCG
PB
37h phCG
PB
39h phCG
PB
B
Experimental Setup:
~ 30h phCG
DMSO/
Aphidicolin
12h
+/- BrdU
42h phCG
48h phCG
RNA extraction
BrdU revelation
DNA FISH
C
DAPI BrdU
DMSO
Aphidicolin
PB
42h phCG
D
Real-Time PCR
quantification
DMSO
Aph
Expression relative to DMSO control
1,5
1
0,5
0
Maj Fwd
Maj Rev
42h phCG
E
DNA FISH
DAPI telomeres major satellites
DMSO
Aphidicolin
PB

Figure 4

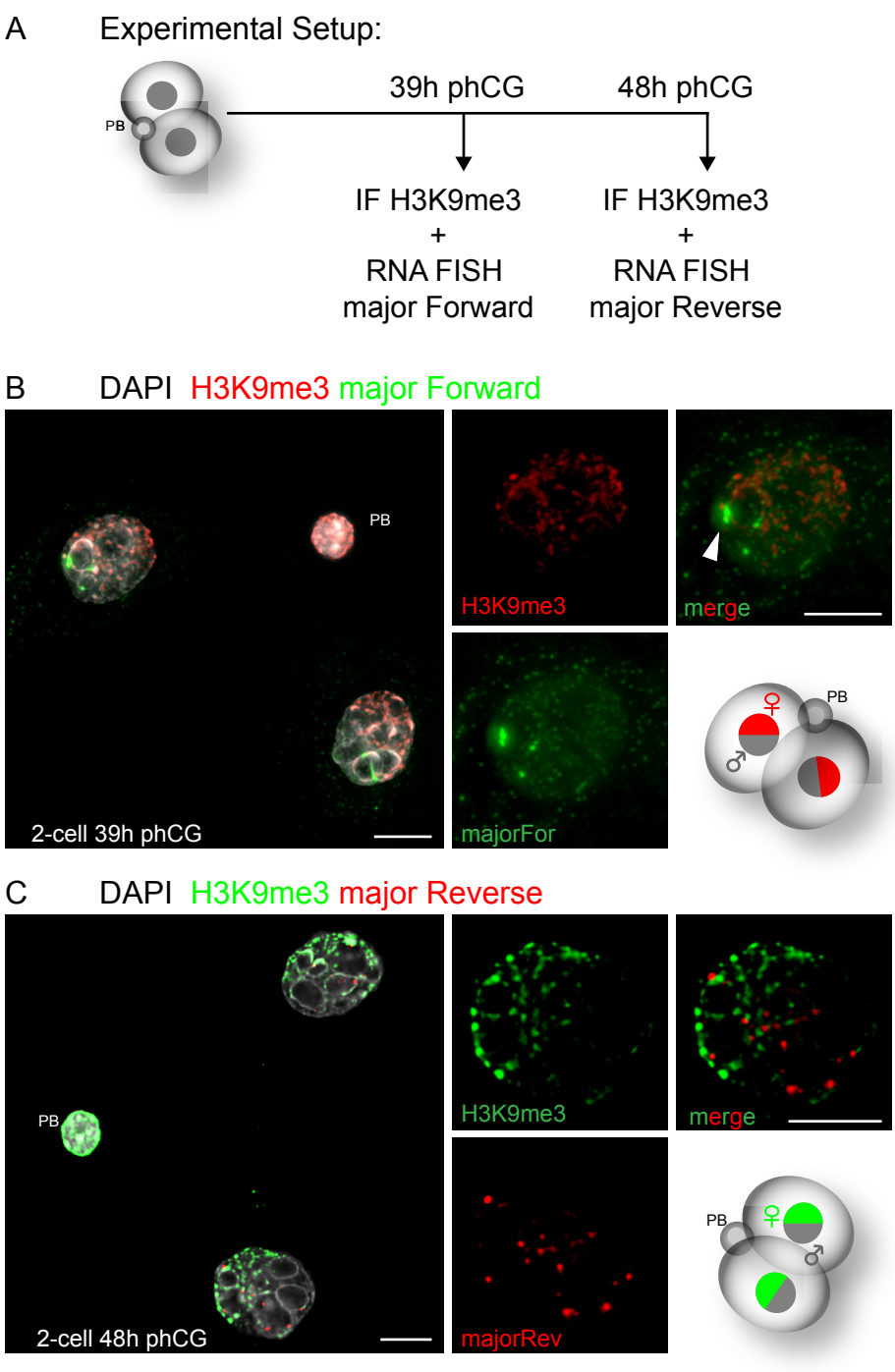
A
Experimental Setup:
PB
39h phCG
48h phCG
IF H3K9me3
+
RNA FISH
major Forward
IF H3K9me3
+
RNA FISH
major Reverse
B
DAPI H3K9me3 major Forward
PB
2-cell 39h phCG
H3K9me3
merge
majorFor
♀
♂
PB
C
DAPI H3K9me3 major Reverse
PB
2-cell 48h phCG
H3K9me3
merge
majorRev
PB
♀
♂

Figure 5

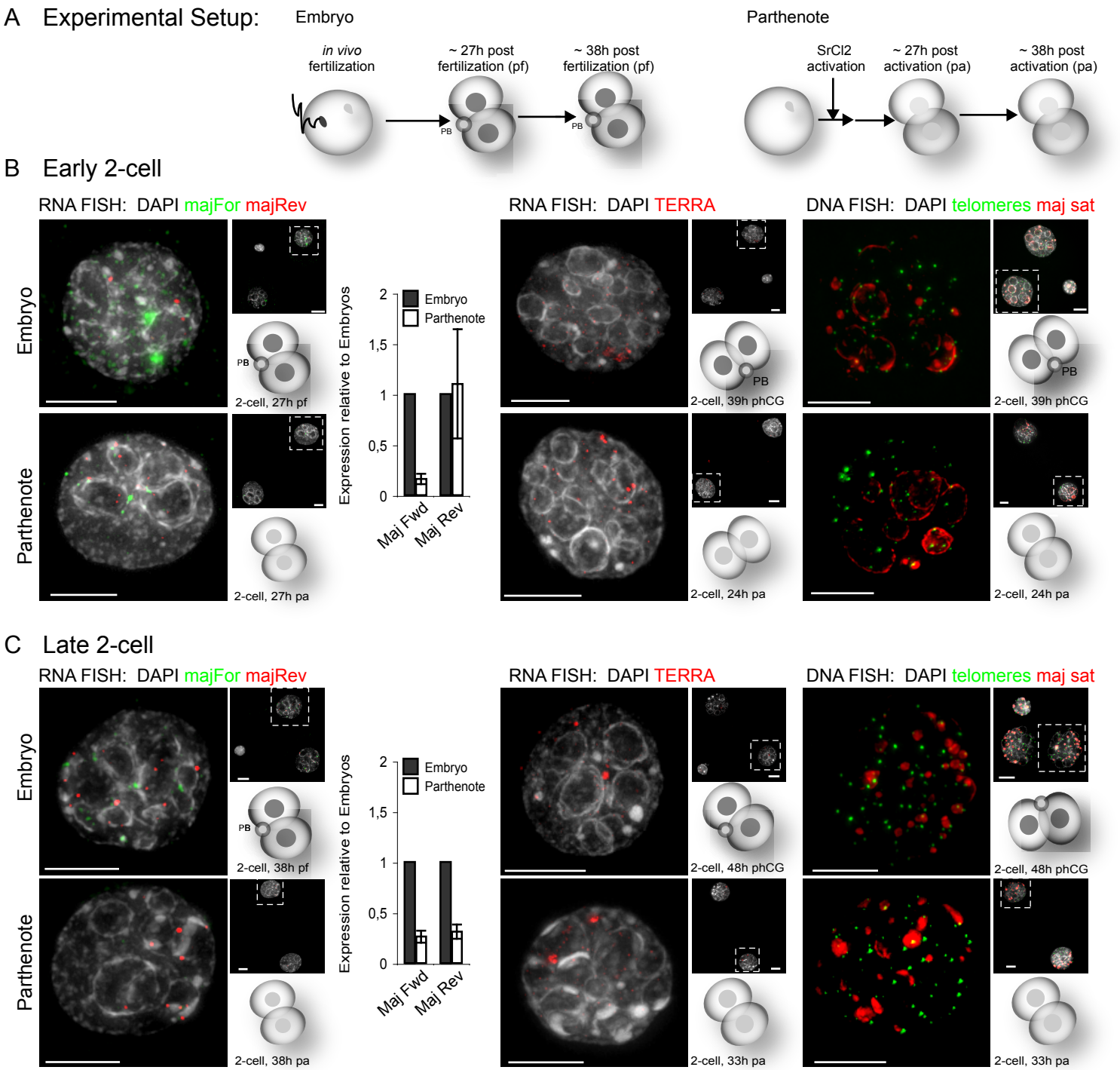
A Experimental Setup:
Embryo
in vivo fertilization
~ 27h post fertilization (pf)
~ 38h post fertilization (pf)
PB
Parthenote
SrCl2 activation
~ 27h post activation (pa)
~ 38h post activation (pa)
B Early 2-cell
RNA FISH: DAPI majFor majRev
RNA FISH: DAPI TERRA
DNA FISH: DAPI telomeres maj sat
Embryo
Parthenote
2-cell, 27h pf
2-cell, 27h pa
2-cell, 39h phCG
2-cell, 24h pa
Expression relative to Embryos
Embryo
Parthenote
Maj Fwd
Maj Rev
C Late 2-cell
2-cell, 38h pf
2-cell, 38h pa
2-cell, 48h phCG
2-cell, 33h pa
D Real-Time PCR quantification - Comparison Embryos and Parthenotes
Expression of major satellites relative to MII oocytes
Parthenote Fwd
Parthenote Rev
Embryo Fwd
Embryo Rev
MII oocytes
1-cell
2-cell 24h pa
2-cell 33h pa
4-cell
8-cell

Figure 6

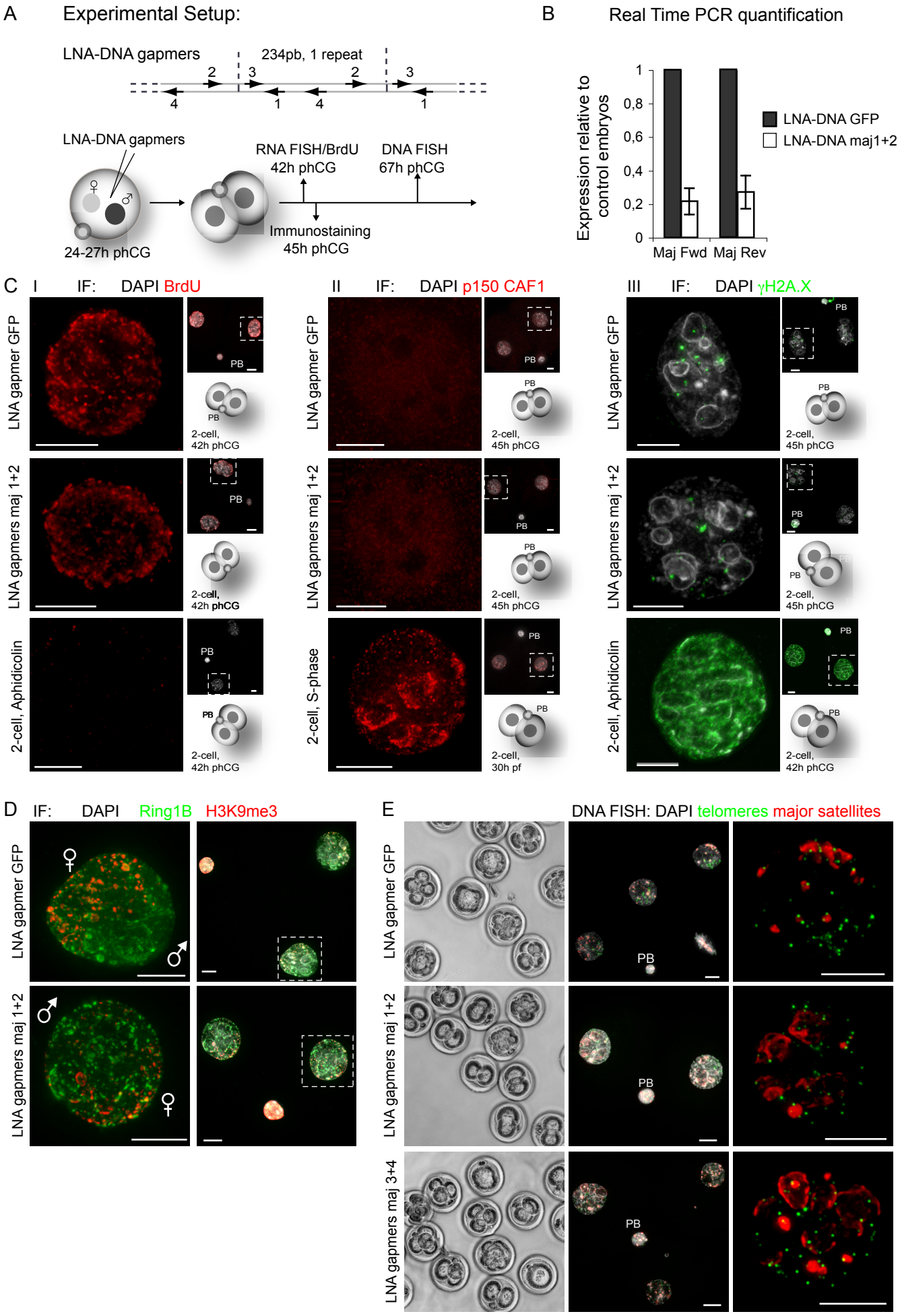
A
Experimental Setup:
LNA-DNA gapmers
234pb, 1 repeat
2
3
2
3
4
1
4
1
LNA-DNA gapmers
RNA FISH/BrdU
42h phCG
DNA FISH
67h phCG
Immunostaining
45h phCG
24-27h phCG
B
Real Time PCR quantification
Expression relative to control embryos
1
0,8
0,6
0,4
0,2
0
LNA-DNA GFP
LNA-DNA maj1+2
Maj Fwd
Maj Rev
C
I
IF:
DAPI BrdU
II
IF:
DAPI p150 CAF1
III
IF:
DAPI γH2A.X
LNA gapmer GFP
LNA gapmers maj 1+2
2-cell, Aphidicolin
2-cell, S-phase
PB
2-cell, 42h phCG
2-cell, 45h phCG
2-cell, 30h pf
D
IF:
DAPI
Ring1B
H3K9me3
LNA gapmer GFP
LNA gapmers maj 1+2
E
DNA FISH: DAPI telomeres major satellites
LNA gapmer GFP
LNA gapmers maj 1+2
LNA gapmers maj 3+4
PB

SUPPLEMENTAL INFORMATION

Figure S1, related to Figure 2

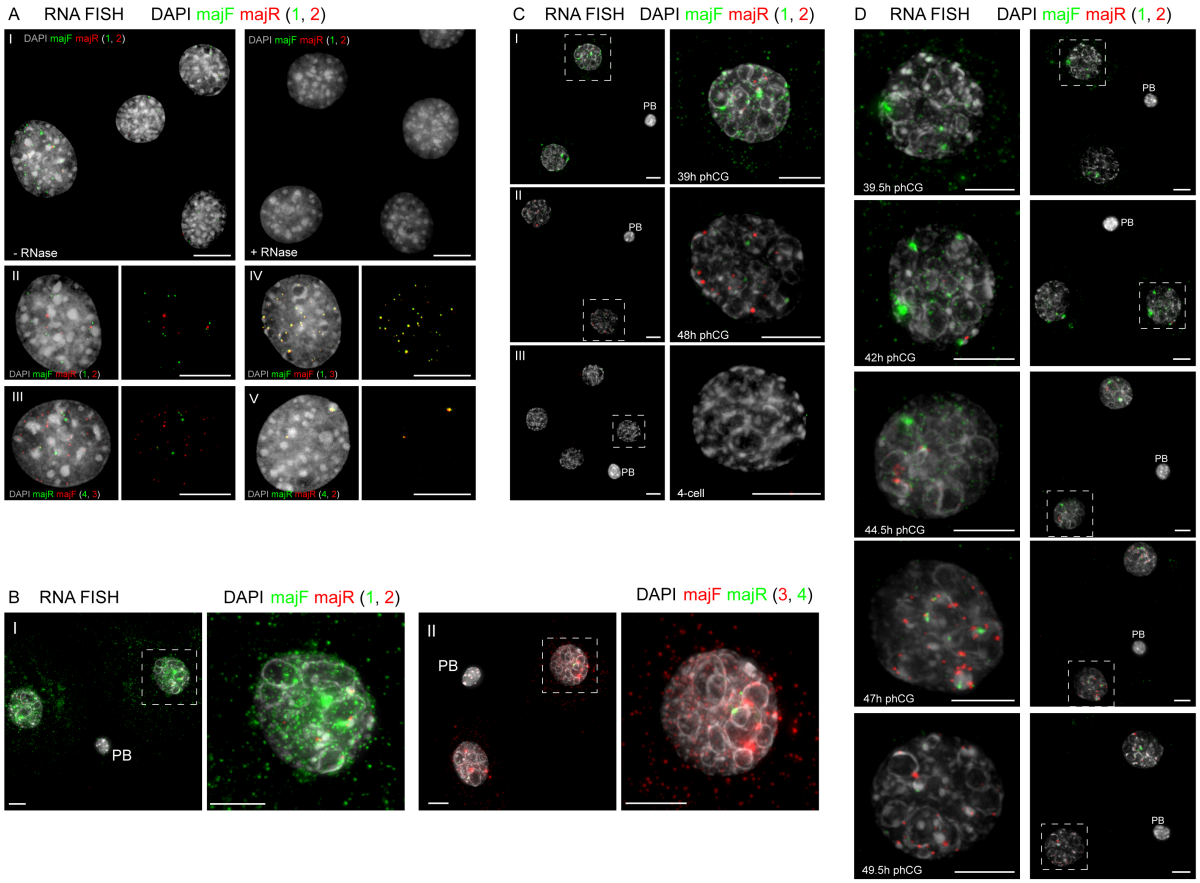

Figure S1, related to Figure 2:

Specific LNA probes reveal discrete expression dynamics of the two complementary major satellite transcripts during the first cleavage stages.

(A) **Strand-specific LNA probes allow unambiguous detection of major RNA.** RNA FISH for major transcripts in 3T3 cells. (I) Field of cells mock (left) or RNase A (right) treated prior to hybridization with strand specific LNA probes (see Figure 2A) 1 and 2. Lack of signals in RNase A treated cells confirms absence of cross-reaction with DNA. Hybridization with probe set 1 + 2 (II) and probe set 3 + 4 (III) results in identical patterns. Yellow signals (co-localization) are obtained, when Forward (probe 1 and 3, IV) or Reverse transcripts (probe 2 and 4, V) are simultaneously detected with a FITC and a Cy3 labeled probe, confirming specificity of the probes. Right panels show the same nucleus in the green and red channel only.

(B) **Forward transcripts are exported to the cytoplasm during the early 2-cell stage.** Early 2-cell embryos (~39h phCG) subjected to RNA FISH using probe set 1 + 2 (I) and 3 + 4 (II). Both probe sets reveal identical patterns and confirm the presence of Forward transcripts in the cytoplasm. Right panels show enlargements of one blastomere nucleus.

(C) **The observed expression dynamics during the first cleavage stages are not a consequence of *in vitro* culture.** Early (39h phCG, I) and late (48h phCG, II) 2-cell embryos as well as 4-cell (III) embryos fixed directly after isolation from the oviduct were processed for RNA FISH with LNA probes specific for the Forward (green) and the Reverse (red) strand of major satellites.

(D) **Analysis of expression of major satellites at different time points during late S/G2-phase of the 2-cell stage reveals a progressive decrease in Forward and an increase in Reverse transcripts, respectively.** RNA FISH with LNA probes specific for the Forward (green) and the Reverse (red) strand of major satellites. Note the simultaneous expression of both transcripts during a certain time window.

DNA is counterstained with DAPI (grey). PB, polar body. Scale bars, 10mM.

Figure S2, related to Figure 3

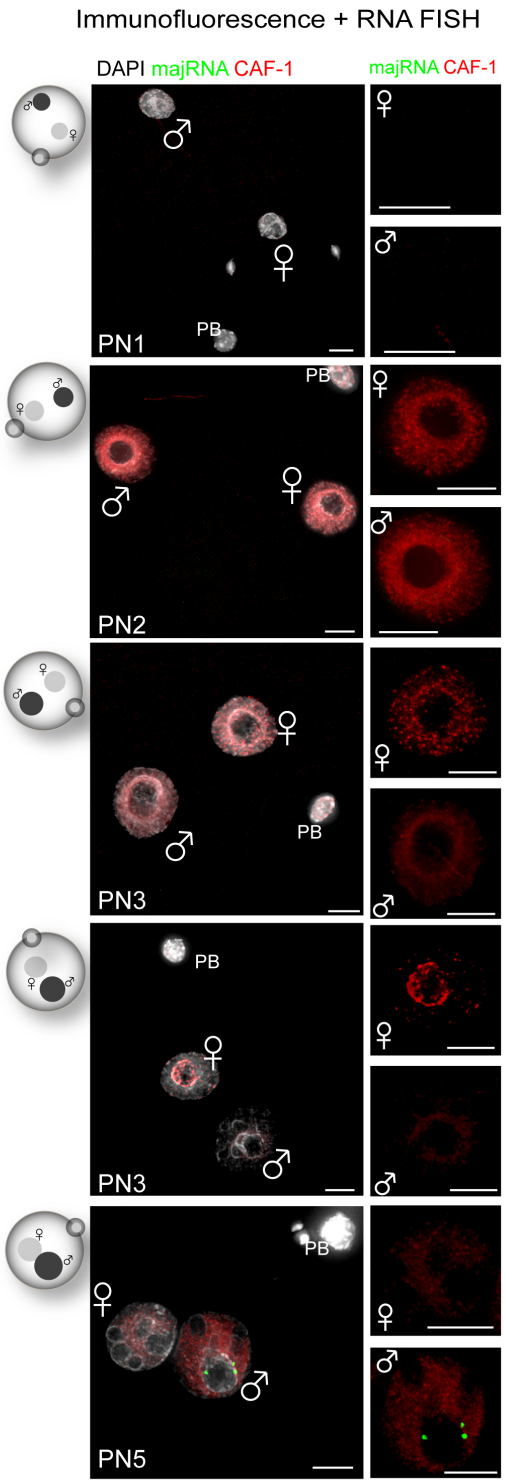

Figure S2, related to Figure 3:

In zygotes, the two parental pronuclei show distinct DNA replication patterns and expression of major satellites.

Following immunodetection of p150 (largest subunit of the CAF-1 complex, red) zygotes at different pronuclear (PN) stages were processed for RNA FISH of major satellites (Forward + Reverse, green). Right panels show enlargements of the two pronuclei in the red and green channel only. Just in the maternal pronucleus clear replication foci are discernable (PN2 and PN3 embryos). This underlines the distinct chromatin environment between the two pronuclei. Major satellite transcripts are detectable in the paternal pronucleus of G2 staged zygotes (last panel). DNA is counterstained with DAPI (grey). Scale bars, 10mM. PB, polar body.

Figure S3, related to Figure 5

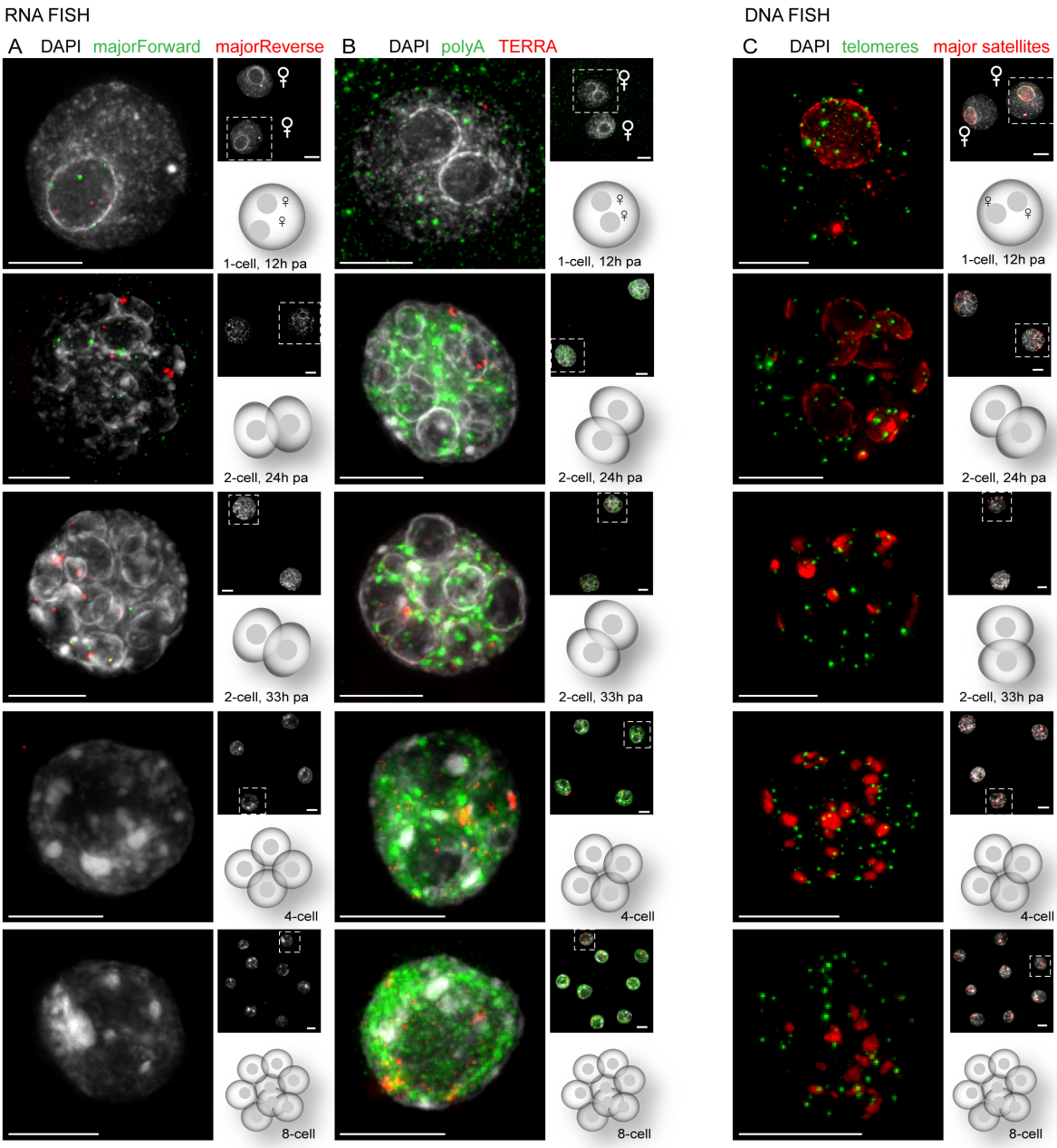
RNA FISH
A DAPI majorForward majorReverse
B DAPI polyA TERRA
DNA FISH
C DAPI telomeres major satellites
1-cell, 12h pa
2-cell, 24h pa
2-cell, 33h pa
4-cell
8-cell

Figure S3, related to Figure 5:

Distinct expression patterns in diploid parthenotes compared to embryos are specific to major satellites and are not observed for TERRA or polyA-RNA.

(A-C) 1-cell, early and late 2-cell, 4-cell and 8-cell parthenotes subjected to RNA or DNA FISH. (A) Major transcripts detected by strand-specific LNA probes: Forward (green) and Reverse (red). (B) Co-detection of bulk poly-adenylated RNA (green) with TERRA (red). The expression patterns of polyA-RNA and TERRA transcripts are identical in parthenotes and embryos (compare to Figure 2 and Figure 5). This argues either that their expression is independent of the parental origin or that in parthenotes compensatory mechanisms are at work, which operate to achieve the global transcriptional activity required for development. In contrast, major satellite transcripts were detected to significantly lower levels in 2-cell parthenotes compared to embryos at the corresponding developmental stages (Figure 5). (C) DNA FISH for major satellites (red) and telomeres (green). As expected from the known reorganization of pericentric satellites in the maternal pronucleus (Probst et al., 2007), both female pronculei in parthenotes reorganize their pericentric domains into ring-like structures around the pro-nucleolar bodies (Martin et al., 2006; Merico et al., 2007). This argues for the existence of a developmental stage-specific spatial organization of the pericentric domains that is initially independent of the parental origin and the epigenetic marks associated with the domains. The ring-structures are progressively resolved into chromocenters during the 2-cell stage and likewise to the organization in embryos, frequent Rabl-like configurations are observed in parthenotes (Merico et al., 2007). Enlargements show one representative blastomere nucleus.

DNA is counterstained with DAPI (grey). PB, polar body. Scale bars, 10mm. pa, post-activation.

Figure S4, related to Figure 6

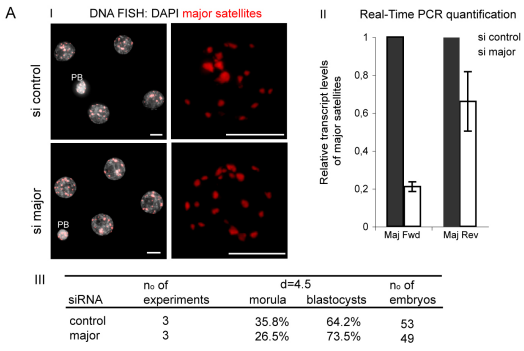

III

siRNA	nº of experiments	d=4.5 morula	d=4.5 blastocysts	nº of embryos
control	3	35.8%	64.2%	53
major	3	26.5%	73.5%	49

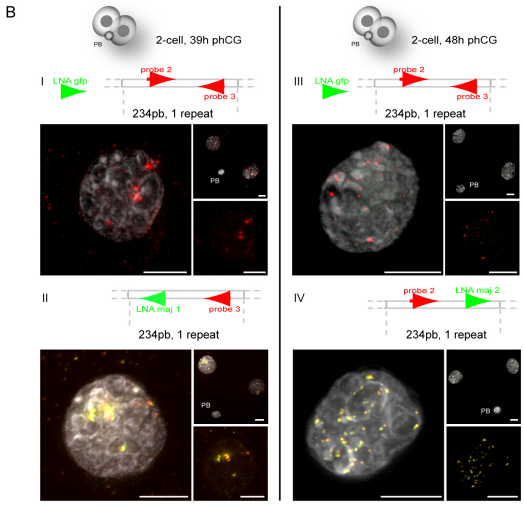

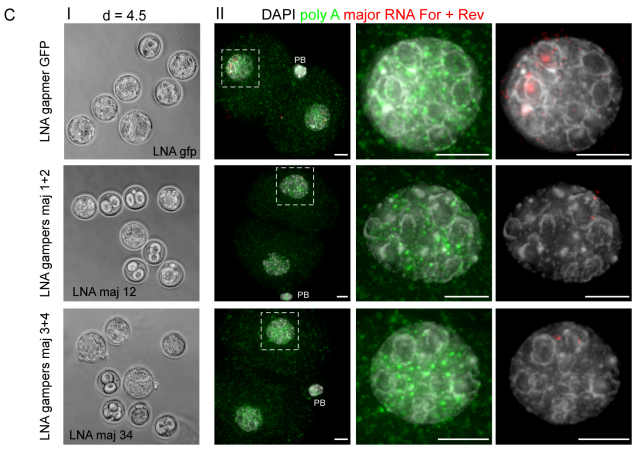

Figure S4, related to Figure 6:

LNA-DNA gapmers allow efficient and specific depletion of major satellite transcripts from pre-implantation embryos.

(A) **Microinjection of siRNAs directed against major satellites does not efficiently deplete Reverse major satellite transcripts.** Zygotes were microinjected between 24-27h phCG with control siRNAs or a mix of siRNAs directed against major satellites and cultured *in vitro*. (I) At the 4-cell stage embryos were subjected to DNA FISH for major satellites (red). Right panels show enlarged images of one representative nucleus in the red channel only. (II) RNA was extracted 42h phCG, reverse transcribed and the amount of major transcripts quantified by quantitative Real-Time PCR. Mean fold changes +/- SD of major RNA in sicontrol (set to 1) and simajor microinjected embryos normalized to U1 RNA are shown. (III) Percentage of embryos having reached morula or blastocyst stage at d=4.5 in sicontrol or simajor injected populations.

(B) **Fluorescently-labeled LNA-DNA gapmers 1 and 2 directed against major RNA specifically recognize the respective major transcripts in RNA FISH assays**. Co-detection of major Forward transcripts in early 2-cell embryos (II) by FAM-labeled LNA-DNA gapmer 1 (green) as well as Reverse transcripts in late 2-cell embryos (IV) by FAM-labeled LNA-DNA gapmer 2 (green) together with Cy3-labelled LNA probes (2 and 3) as indicated. The FAM-labeled LNA-DNA gapmer directed against GFP (green, I, III) does not result in nonspecific hybridization to major transcripts.

(C) **Embryos microinjected with LNA-DNA gapmers directed against major transcripts show reduced major satellites transcripts, but an unaltered polyA RNA expression pattern by 42h phCG**. (I) Bright field images of microinjected embryos at d=4.5. (II) Zygotes were microinjected either with LNA-DNA gapmers directed against GFP or with a set of two LNA-DNA gapmers directed against Forward and Reverse major transcripts. Embryos were fixed ~ 42h phCG and processed for RNA FISH using probes for major satellites (red) and bulk polyA RNA (green). Middle and right panels show enlargement of one blastomere nucleus.
DNA is counterstained with DAPI (grey). Scale bars, 10mM. PB, polar body.

Figure S5

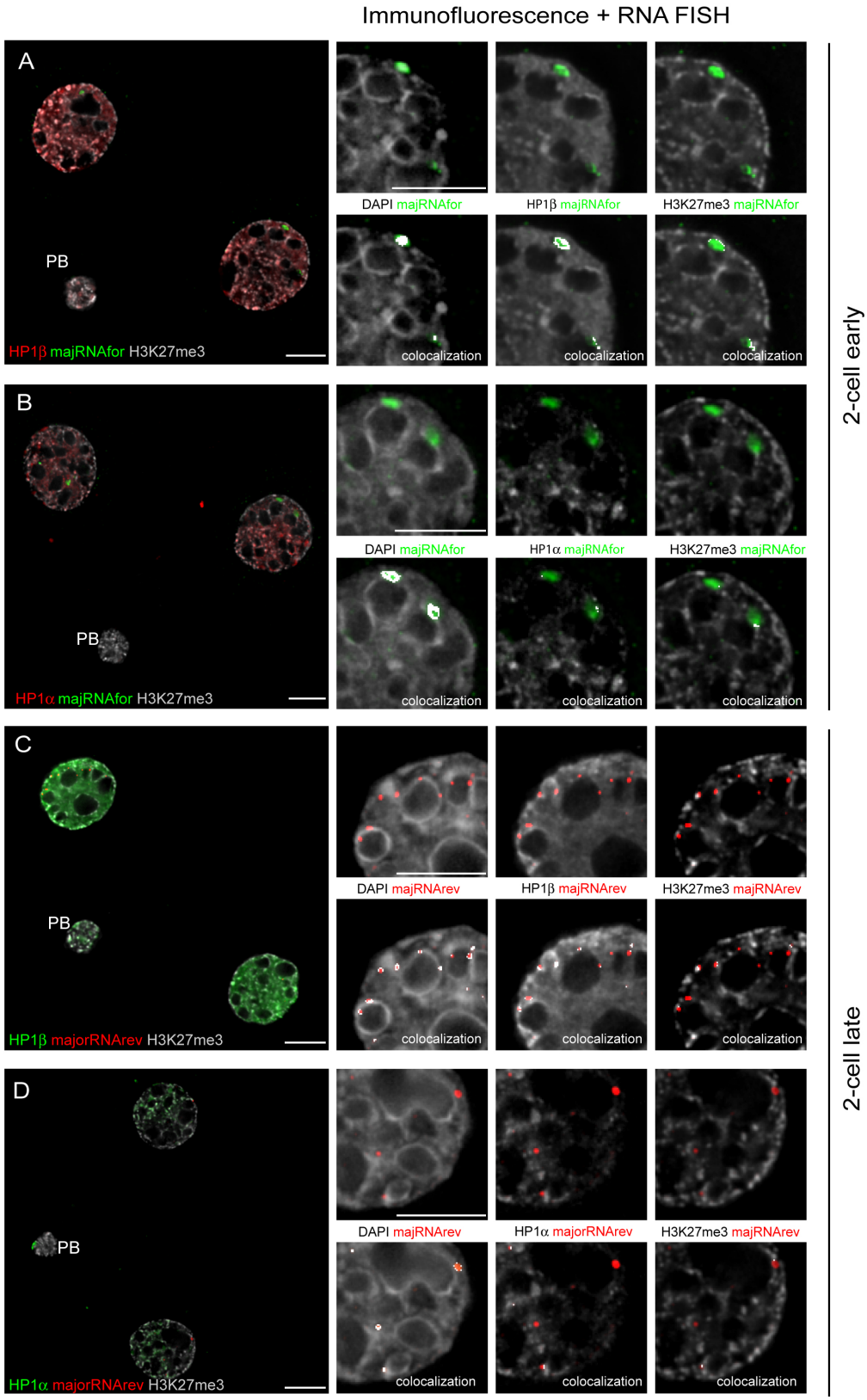
Immunofluorescence + RNA FISH
A
PB
HP1β majRNAfor H3K27me3
DAPI majRNAfor
HP1β majRNAfor
H3K27me3 majRNAfor
colocalization
colocalization
colocalization
B
PB
HP1α majRNAfor H3K27me3
DAPI majRNAfor
HP1α majRNAfor
H3K27me3 majRNAfor
colocalization
colocalization
colocalization
2-cell early
C
PB
HP1β majorRNArev H3K27me3
DAPI majRNArev
HP1β majRNArev
H3K27me3 majRNArev
colocalization
colocalization
colocalization
D
PB
HP1α majorRNArev H3K27me3
DAPI majRNArev
HP1α majorRNArev
H3K27me3 majRNArev
colocalization
colocalization
colocalization
2-cell late

Figure S5:

Forward transcripts show limited co-localization with HP1b, but not HP1a or H3K27me3 in early 2-cell embryos.

Single optical sections of early (39h phCG) and late (48h phCG) 2-cell embryos. Following immunodetection of HP1β (A, C), HP1α (B, D) and H3K27me3 (as mark for Polycomb mediated silencing) (A-D), embryos were processed for RNA FISH. Strand-specific probes reveal Forward (green, A, B) in early 2-cell and Reverse transcripts (red, C, D) in late 2-cell embryos. Combinations of antibodies and RNA FISH probes were applied as indicated in the Figure. Left panels show the whole embryo. Right panels show enlargements of part of one blastomere nucleus with DAPI or immunostaining in grey and RNA FISH signals in green or red. In lower panels co-localization as determined by the Colocalization plugin in ImageJ made available by Pierre Bourdoncle, Institut Jacques Monod, Paris is indicated in white. Scale bars, 10mM.

The Forward transcripts accumulate on DAPI-bright rings. HP1α follows the distribution of H3K9me3 and is only poorly enriched at the paternally derived part of the genome and the area coated by the Forward strand. HP1β, even though enriched in the maternal genome, is present throughout the nucleus and also colocalizes with Forward transcripts. The Reverse transcripts localize to the DAPI-bright areas, but reveal no co-localization with H3K27me3 and partial co-localization with HP1α and β.

Table S1:

Expression of major satellite transcripts in zygotes

RNA FISH signals per zygote		
only in paternal pronucleus	**in both pronuclei**	**n**
76%	24%	42

n = number of zygotes analyzed

Table S2:

Expression of major satellite transcripts in 1-cell parthenotes

RNA FISH signals per 1-cell parthenote		
only in one of the 2 pronuclei	**in both pronuclei**	**n**
12.5%	87.5%	16

n = number of 1-cell parthenotes analyzed

Table S3:

Expression of Forward and Reverse transcripts in zygotes and 1-cell parthenotes

	Percentage of zygotes or 1-cell parthenotes with higher number of Reverse transcript signals than Forward signals	**n**
Zygotes	80%	10
1-cell parthenotes	44%	16

n = number of zygotes and 1-cell parthenotes analyzed

In embryos, exclusive paternal expression of major satellite transcripts was observed in 76% of the zygotes (n=42, Table S1). These data are in agreement with the increased transcriptional competence of the paternal versus the maternal pronucleus that has been described before (Aoki et al., 1997; Bouniol et al., 1995) and the predominant expression of major satellites in the paternal pronucleus reported by (Puschendorf et al., 2008). The difference in expression patterns between the two pronuclei is specific to embryos, in which the two parental genomes show distinct chromatin modifications, since in 87,5% of the 1-cell parthenotes (n=16, Table S2) we observed expression of major satellites in both pronuclei.

In 8 out of 10 zygotes more signals corresponding to Reverse than Forward transcripts were found confirming the predominant expression of the Reverse strand in the paternal pronucleus of the zygote. Furthermore, in parthenotes, the number of signals observed for Forward and Reverse transcripts were similar (only 44% showed more Reverse transcripts compared to 80% in zygotes, n=16, Table S3).

SUPPLEMENTAL EXPERIMENTAL PROCEDURES

Antibodies and siRNAs

For immunostaining we used the following antibodies: polyclonal anti-CAF-1p150 (Quivy et al., 2004) (AgroBio, 1:500), monoclonal anti-HP1a (Euromedex, 1:400), monoclonal anti-HP1b (Euromedex, 1:400) and polyclonal anti-H3K27me3 (Upstate, 1:200) in combination with highly cross-absorbed Alexa 488, 594 or 647-coupled secondary antibodies (1:800) from Molecular Probes. We purchased siRNAs targeting the following sequences within major repeats CACTGTAGGACGTGGAATA, CCATATTTCACGTCCTAAA and GCAAGAAAACTGAAAATCA and for negative control AAGCGCGCTTTGTAGGATTCG from Dharmacon and FAM-labeled LNA-DNA gapmers from Exiqon.

Sequence of Probes, LNA-DNA gapmers and primers

Name	Fluorophore	Sequence (LNA nucleotides in lower case letters where known)
major 1	FITC	TCTTGCCATATTCCACGTCC
major 2	Cy3	GCGAGGAAAACTGAAAAAGG
major 3	Cy3	GATTTCGTCATTTTTCAAGT
major4	FITC	GCGAGAAAACTGAAAATCAC
TERRA	Cy3	CCCTAACCCTAACCCTAACCCTAACCCTAACCCTAA
Telomere DNA FISH	6-Fam	GGGTTAGGGTTAGGGTTAGGGTTAGGGTTAGGGTTA
LNA DNA gapmer maj 1	-	acatCCACTTGACGActtg
LNA DNA gapmer maj 2	-	tattTCACGTCCTAAagtg
LNA DNA gapmer maj 3	-	cgagAAAACTGAAAAtcac
LNA DNA gapmer maj 4	-	cataTTCCAGGTCCTtcag
LNA DNA gapmer gfp	-	gagaAAGTGTGACAagtg
LNA DNA gapmer control	-	gcgcGCTTTGTAGGAttcg
LNA DNA gapmer maj 1	FAM	acatCCACTTGACGActtg
LNA DNA gapmer maj 2	FAM	tattTCACGTCCTAAagtg
LNA DNA gapmer gfp	FAM	gagaAAGTGTGACAagtg
RT- PCR primer F	-	GACGACTTGAAAAATGACGAAATC
RT- PCR primer R	-	CATATTCCAGGTCCTTCAGTGTGC

Cell culture

We grow mouse NIH 3T3 cells (ATCC) in DMEM supplemented with 10% FCS, 10mg/mL penicillin and streptomycin (GIBCO).

Embryo culture and siRNA microinjection

Zygotes from superovulated females were microinjected with siRNA (20mM) mix in 1x siRNA buffer (Dharmacon) and cultivated in microdrops of M16 medium (Sigma) at 37°C under 5% CO_2.

Immunofluorescence, RNA and DNA FISH

Embryos: After removal of the zona pellucida with acidic Tyrode's Solution (Sigma), mouse embryos were dried on coverslips coated with Denhardt solution (Okamoto et al., 2004). We fixed the embryos in 3% PAF for 12min, permeabilized them in 0.5% Triton X-100 in PBS supplemented with 10mM Vanadyl ribonucleoside complex (VRC, NEB) for 4.5 – 6min on ice depending on the developmental stage and stored them in 70% EtOH at -20°C overnight. Following dehydration in 80%, 95% and 100% EtOH, we carried out hybridization with fluorescently labeled LNA probes as indicated (Exiqon) at 0.4mM in 50% Formamide (Sigma), 2x SSC (Sigma), 10% Dextran Sulfate (Fluka), 10mM VRC and 2mg/mL BSA (NEB) for 35min at 37°C. After 3 washes for 5min in 0.1x SSC at 60°C, we stained with DAPI and mounted the embryos in Vectashield (Vector Laboratories). Immuno-RNAFISH was performed as in (Chaumeil et al., 2008) with the following minor modifications: following post-fixation, embryos were stored overnight in 70% EtOH at -20°C. DNA FISH on cells and embryos was performed as described (Guenatri et al., 2004; Probst et al., 2007), except that the hybridization mix contained LNA oligonucleotide probes (0.1mM) and post-hybridization washes were in 0.1x SSC (3 x 5min) at 60°C.

To confirm specificity of LNA-DNA gapmers we used FAM-labeled gapmers as RNA probe (final concentration in RNA hybridization buffer was 0.4 mM).

Cultured cells: After extraction with 0.5% Triton X-100 in CSK buffer (10mM Pipes pH7, 100mM NaCl, 300mM sucrose, 3mM $MgCl_2$ (Martini et al., 1998), supplemented with 10mM Vanadyl ribonucleoside complex (VRC) for 5min on ice, we fixed 3T3 cells in 3% Paraformaldehyde in PBS for 12min and stored them in 70% EtOH at -20°C overnight. Following dehydration in 80%, 95% and 100% EtOH, we carried out hybridization with fluorescently labeled LNA probes as described for embryos. For RNase treatment prior to hybridization, we rehydrated cells in 2x

SSC and treated with RNase A (0.1 mg/mL in 2x SSC) for 1h at 37°C. After 3 washes in 2x SSC, cells were dehydrated and processed for RNA FISH as described.

RNA isolation and RT-PCR analysis

We used Trizol (Invitrogen) to extract RNA from cells and embryos. For Reverse transcription of RNA extracted from embryos injected with siRNAs we used strand specific primers: major F: GACGACTTGAAAAATGACGAAATC, major R: CATATTCCAGGTCCTTCAGTGTGC and U1: CAGTCCCCCACTACCACAAA. We performed Real-Time PCR using LightCycler FastStart DNA Master^{Plus} Sybr Green I (Roche) in a Roche LightCycler or Power SYBR Green (Applied Biosystems) with the ABI 7500 Fast Real-TIME PCR System for major satellites as in (Terranova et al., 2005) and with the combination For: CTTACCTGGCAGGGGAGATA and Rev: CAGTCCCCCACTACCACAAA for U1.

SUPPLEMENTAL REFERENCES

Chaumeil, J., Augui, S., Chow, J.C., and Heard, E. (2008). Combined immunofluorescence, RNA fluorescent in situ hybridization, and DNA fluorescent in situ hybridization to study chromatin changes, transcriptional activity, nuclear organization, and x-chromosome inactivation. Methods Mol Biol *463*, 297-308.

Martin, C., Beaujean, N., Brochard, V., Audouard, C., Zink, D., and Debey, P. (2006). Genome restructuring in mouse embryos during reprogramming and early development. Dev Biol *292*, 317-332.

Martini, E., Roche, D.M., Marheineke, K., Verreault, A., and Almouzni, G. (1998). Recruitment of phosphorylated chromatin assembly factor 1 to chromatin after UV irradiation of human cells. J Cell Biol *143*, 563-575.